Electric Spring and Smart Load: Technology, System-Level Impact, and Opportunities

Chi-Kwan Lee, *Senior Member, IEEE*, Heng Liu, Siew-Chong Tan, *Senior Member, IEEE*, Balarko Chaudhuri, *Senior Member, IEEE*, and Shu-Yuen Ron Hui, *Fellow, IEEE*

(Invited Paper)

***Abstract*— The increasing use of renewable energy sources to combat climate change comes with the challenge of power imbalance and instability issues in emerging power grids. To mitigate power fluctuation arising from the intermittent nature of renewables, electric spring (ES) has been proposed as a fast demand-side management technology. Since its original conceptualization in 2011, many versions and variants of ESs have emerged and industrial evaluations have begun. This article provides an update of the existing ES topologies, their associated control methodologies, and studies from the device level to the power system level. Future trends of ESs in large-scale infrastructures are also addressed.**

***Index Terms*— Demand response, demand-side management (DSM), distributed renewable generations, electric spring (ES), smart load (SL).**

NOMENCLATURE

AC-ES	AC electric spring.
BTB	Back-to-back.
CL	Critical load.
DCES	DC electric spring.
D-FACT	Distributed flexible ac transmission.
D-STATCOM	Distributed static VAR compensator.
DSM	Demand-side management.
ES	Electric spring.
EVs	Electric vehicles.
EWH	Electric water heater.
H-DCES	Hybrid dc electric spring.
HVAC	Heating, ventilations, and air-conditioning.
LV	Low voltage.
NCL	Noncritical load.
PLL	Phase-locked loop.
P_{CL}	Power of critical load.
P_{NCL}	Power of noncritical load.
PV	Photovoltaic.
RCD	Radial–chordal decomposition.
R/X	Resistance/reactance.
SL	Smart load.
SOC	State-of-charge.
TCL	Thermostatically controlled loads.
V_s	AC mains voltage.
V_{ES}	Voltage across the electric spring.
V_{NC}	Voltage across the noncritical load.

Manuscript received March 23, 2020; revised May 21, 2020; accepted June 16, 2020. Date of publication June 22, 2020; date of current version December 1, 2021. Recommended for publication by Associate Editor Xiongfei Wang. *(Corresponding author: Shu-Yuen Ron Hui.)*

Chi-Kwan Lee, Heng Liu, and Siew-Chong Tan are with the Department of Electrical and Electronic Engineering, The University of Hong Kong, Hong Kong.

Balarko Chaudhuri is with the Department of Electrical and Electronic Engineering, Imperial College London, London SW7 2AZ, U.K.

Shu-Yuen Ron Hui is with the Department of Electrical and Electronic Engineering, The University of Hong Kong, Hong Kong, and also with the Department of Electrical and Electronic Engineering, Imperial College London, London SW7 2BU, U.K. (e-mail: ronhui@eee.hku.hk).

Color versions of one or more of the figures in this article are available online at https://ieeexplore.ieee.org.

Digital Object Identifier 10.1109/JESTPE.2020.3004164

I. INTRODUCTION

THE rapid contraction of sea ice in the Arctic [1] and Antarctica [2], huge bush fires in Amazon forest [3] and Australia [4], atmospheric CO_2 concentration passing 400 ppm, and continual rising of acidity of seawater, sea level, and global temperature [5] have prompted urgent needs to address the climate change issues. Renewable energy, clean energy conversion, energy storage, nuclear energy, carbon capture and sequestration, replacement of combustion vehicles with electric ones, and sustainable building designs are parts of the existing solutions to combat climate change. Based on the 2019 data provided by the International Renewable Energy Agency (IRENA) [6], solar power (94 GW; +24% over 2017) and wind power (49 GW; +10% over 2017) are the top two dominant renewable energy capacities installed in 2018.

The increasing use of wind and solar power of intermittent nature poses new challenges to power system stability, which requires an instantaneous balance of power supply and load demand. In fact, intermittent renewables will not only lead to power system collapse [7] but also the instability problems may even be exported to the neighboring countries with power networks connected to the same super grid [8]. The traditional power systems adopt the centralized generation principle with the control paradigm of "power generation (supply) following load demand" and unidirectional power flow from the power stations to the load centers. With increasing capacities of the distributed renewable energy generation, the control paradigm for centralized power generation is no longer valid for the future power grid. The distributed renewable energy generation in the load centers implies bidirectional power flow in the power networks and renewable power generation has stochastic nature. Therefore, for an emerging power grid, there is a need for a radical change in the control paradigm to "load demand following power generation" to achieve power balance for system stability. The key differences between the traditional and emerging power grids are highlighted in Table I.

TABLE I
KEY DIFFERENCES BETWEEN TRADITIONAL AND EMERGING POWER SYSTEMS

Traditional Power Generation	**Emerging Power Generation**
Centralized	Distributed
Unidirectional power flow	Bidirectional power flow
Traditional Control Paradigm	**New Control Paradigm**
Power generation (supply) follows load demand	Load demand follows power generation (supply)

Demand response or DSM is not a new concept [9]. Power companies have been using the traditional demand response methods such as 1) scheduling of deferrable loads (e.g., washing machines, dishwashers) [10] and 2) energy storage [11], real-time pricing [12], and direct ON–OFF control of NCLs [13] to alleviate peak demands. Although these methods have their advantages, they have inherent limitations. For example, load scheduling can only be achieved days or hours ahead and cannot provide instantaneous demand response and direct ON–OFF control of customers' loads may cause user inconvenience. Moreover, the traditional demand response methods may not offer solutions even if the overall system power supply and load demand are balanced. For example, excessive PV power injection in local distribution line could cause transient overvoltage [14]. Therefore, fast and distributed demand response methods deserve more attention.

Modern power electronics provides the technology to develop fast demand response solutions to cope with fast fluctuation of renewable power injection into the power grid. This article addresses recent developments in ES technology that has been proposed to enable effective demand response with very fast response time in the order of tens of milliseconds (i.e., almost instantaneous for the power systems at mains frequency of 50 or 60 Hz). Starting with a brief explanation of the ES concept, this article describes various types of ES topologies and their variants reported since 2012 for smart grid applications. For ac power systems, these functions include voltage and frequency regulation, power quality improvement, reduction of power imbalance, reduction of energy storage, and enhancing power system resilience. ESs can also be applied to dc power grid, and the research and developments so far are summarized. Different control schemes corresponding to their circuit topologies proposed by several research groups are then explained. Besides individual control, droop and distributed control of a large group of the distributed ESs are explained. After the ES device aspects have been addressed, recent investigations of ES applications to power systems will be covered. Future trends of ES research are discussed before the conclusion section.

II. CONCEPT OF ES

A mechanical spring is an elastic device that can be used to 1) provide mechanical support; 2) store mechanical energy; and 3) damp mechanical oscillations. When compressed or stretched, it exerts an opposite force proportional to its change in displacement. Potential energy (PE) is stored in the mechanical spring when the length of the spring deviates from its natural length. The principle of the mechanical springs has been described by Hooke [15] in 1678. Hooke's law states that the force of an ideal mechanical spring is

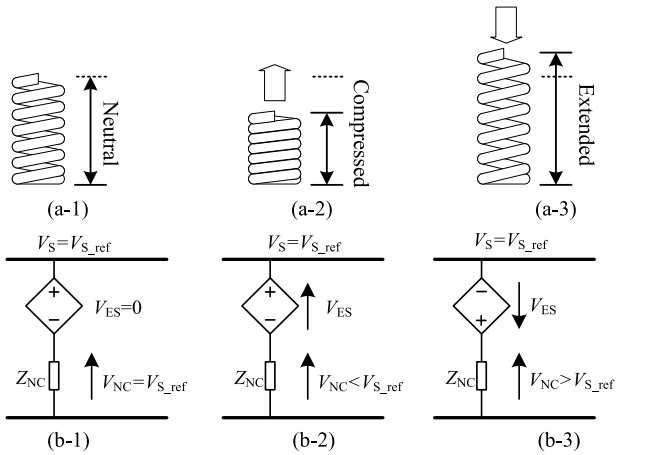

Fig. 1. Similarity between a mechanical spring and an ES. (a-1) and (b-1) Neutral mode. (a-2) and (b-2) Boosting mode. (a-3) and (b-3) Suppression mode [16].

$$\mathbf{F} = -k\mathbf{x} \tag{1}$$

where $\mathbf{F}$ is the force vector, k is the spring constant, and $\mathbf{x}$ is the displacement vector. The PE stored in the mechanical spring is

$$\text{PE} = \frac{1}{2}kx^2. \tag{2}$$

Analogous to a mechanical spring, an ES is an electric device that can be used to 1) provide voltage support; 2) store electric energy; and 3) damp electric oscillations (Fig. 1). Analogous to (1), the basic physical relationship of the ES is expressed as

$$q = \begin{cases} Cv_a & \text{inductive mode} \\ -Cv_a & \text{capacitive mode} \end{cases} \tag{3}$$

where q is the electric charge stored in a capacitor with capacitance C, v_a is the electric potential difference across the capacitor, and i_c is the current flowing into the capacitor (Fig. 2). The energy storage capability of the ES can be seen from the potential electric energy stored in the capacitor

$$\text{PE} = \frac{1}{2}Cv_a^2. \tag{4}$$

So the capacitor C serves as the energy storage element for the ES and the voltage v_a can be considered as the voltage of the ES V_{ES}.

The first article on ES was published in 2012 [16]. Fig. 1 depicts the similarity between a mechanical spring and the simplest form of an ES, in which the ES is represented with a voltage block generating a compensating voltage V_{ES} and connected in series with an NCL Z_{NC}. When the mains voltage V_{S} deviates from its reference value $V_{\text{S\_ref}}$, the ES can operate in different modes to restore V_{S}. In the voltage boosting mode, the ES generates a supporting voltage to boost the mains voltage, while in the voltage suppression mode the ES provides a suppressing voltage to reduce the mains

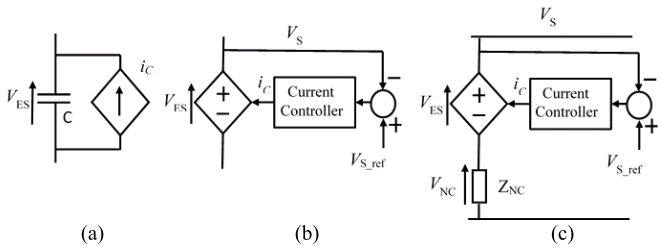

Fig. 2. (a) ES in form of a capacitor fed by a controlled current source. (b) Schematic of an ES with input-feedforward and input voltage control. (c) ES in series with a dissipative load for energy storage, voltage support, and damping.

voltage. In this way, the ES functions as a dynamic voltage restorer damping electric oscillations. V_{ES} can be generated dynamically by controlling the current in a capacitor as shown in Fig. 2.

Two important points about the ES should be noted.

1) Various forms of ES have emerged over the past few years. The basic form of ES provides a standard ac mains voltage well-regulated within its nominal voltage tolerance (e.g., ±5%) and an adaptive ac mains voltage possibly with a higher voltage tolerance (e.g., +10%/−20%). In this case, the standard mains will be used for CLs (Z_C) (that require tight voltage regulation) and the adaptive mains for NCLs (Z_{NC}) (that are tolerant to relatively large mains voltage fluctuation).
2) However, recent research of ES indicates that if the adaptive mains voltage is controlled within the nominal voltage tolerance (e.g., ±5%), the distributed ES can still offer significant active and reactive power compensation and virtual inertia for mitigating mains voltage and frequency fluctuation on a power system level [17], [83]. In this case, there is no need to differentiate electric loads as critical and noncritical. Readers of this article should remember this important point, although the following discussions will start by assuming the CL and NCL classification.

For the ES technology, the electric load Z_{NC} is in series with the output of the ES. The ES and its associated NCL can be considered as a type of SL, which can consume power in an adaptive manner to stabilize the power grid. Such an NCL is used for two reasons. First, the NCL voltage V_{NC} is a necessary component of the dynamic voltage compensation according to Kirchhoff's voltage law (KVL) shown in (5). V_{ES} and V_{NC} have to change simultaneously to maintain V_S to the nominal value within its tight voltage tolerance. Second, the NCL consumes controllable power adaptively based on the variation in the output voltage of ES (i.e., the adaptive mains voltage). The NCL power changes adaptively to absorb the fluctuating power generation to regulate V_S. The vectorial relationship of the mains voltage, ES voltage, and NCL voltage is

$$V_S = V_{NC} + V_{ES}. \tag{5}$$

Generally, electric loads can be classified into two categories: 1) CLs, for example, computers and medical equipment, which require tightly regulated supply voltage, and 2) NCLs, for example, electric heaters and lighting loads, which can tolerate a certain amount of voltage and power variation without significant adverse impact on the loads and consumers. The power consumption of NCL is dependent on its supply voltage. Therefore, it is possible to adjust their power consumption by controlling the voltage. They are suitable candidates to work with ES.

TABLE II
ELECTRICITY CONSUMPTION BY END-USE IN HONG KONG

End use	Residential	Commercial	Industrial
Cooking	9%	7%	---
Air conditioning	35%	29%	27%
Hot water & Refrigeration	22%	8%	---
Lighting	9%	15%	10%
Equipment	15%	6%	41%
Others	10%	35%	22%

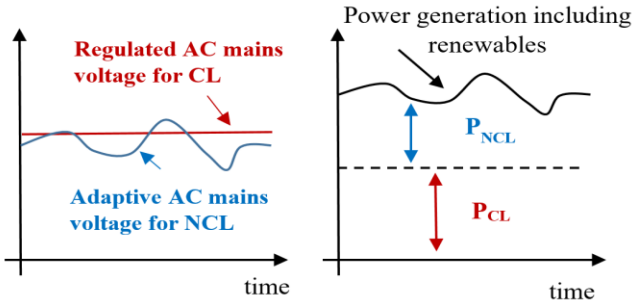

Fig. 3. ES technology for balancing power supply and demand.

NCLs are widely distributed on the demand side and take a relatively high percentage of electricity usage. The electricity consumption by end-use in Hong Kong [18] in 2016 as shown in Table II reports that TCL, which includes HVAC loads (e.g., heating, ventilation, and air-conditioner), EWHs, and refrigerators, account for 27%–57% of the total electricity usage in residential, commercial, and industrial consumption. Similar NCL percentage range has been reported in Singapore [19].

Fig. 3 illustrates the instantaneous power balancing concept of power supply and demand using the ES technology. The ES regulates the standard ac mains voltage for the CL and its output becomes an adaptive ac mains voltage for NCL. The NCL consumes power (P_{NCL}) adaptively to follow the fluctuating power generation profile in real time.

III. CLASSIFICATIONS OF AC-ES

Since the first ES concept appeared in [16], different versions of ES have been proposed. Generally, they can be classified into five categories according to their configurations, namely, 1) the first version of ES-1; 2) the second version of ES with battery storage (ES-2); 3) ES with bidirectional power flow control of battery having nominal SOC of 0.5 (ES-3); 4) BTB ES; and 5) ES integrated with PV panel and other variants. Single-phase ES versions can also be extended to three-phase ES.

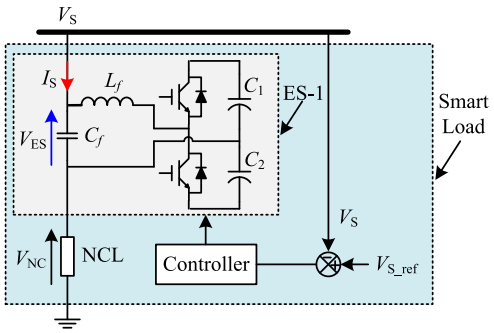

Fig. 4. Schematic of the initial ES-1 based on input voltage control.

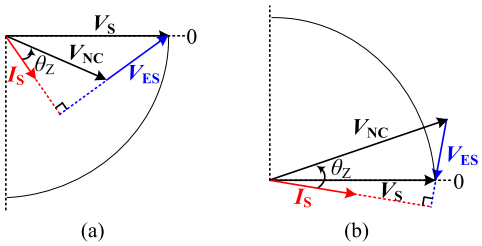

Fig. 5. Vector diagrams of ES-1 in different operation modes. (a) Inductive mode ($+Q_{ES}$). (b) Capacitive mode ($-Q_{ES}$).

A. First ES (ES-1)

The original ES-1 is proposed as a local mains voltage regulator for the power grid with intermittent renewable source generation [20]. Fig. 4 shows a simplified schematic of ES-1 which is implemented with a dc/ac pulsewidth modulation (PWM) inverter with capacitors, C_1 and C_2, on the dc link and an *LC* filter at the output. The PWM inverter can be either a half-bridge or a full-bridge converter. ES-1 and NCL work together as an SL. In the voltage regulation mode, the voltage error between the mains voltage V_S and its reference V_{S_ref} is fed to the ES controller to change the ES voltage V_{ES} until the mains voltage is regulated at its desired value.

The antiparallel diodes of the inverter act as a rectifier to provide a dc voltage across the capacitors C_1 and C_2. ES-1 can provide reactive power compensation. Therefore, the ES-1 voltage vector $\boldsymbol{V_{ES}}$ must be perpendicular to its current vector $\boldsymbol{I_S}$ in the ideal case when the power loss of the ES converter is ignored. $\boldsymbol{V_{ES}}$ can either lead or lag $\boldsymbol{I_S}$. Correspondingly, ES-1 operates in two modes consuming different reactive power Q_{ES}.

1) Inductive mode, $\boldsymbol{V_{ES}}$ leads $\boldsymbol{I_S}$ by 90° ($+Q_{ES}$).
2) Capacitive mode, $\boldsymbol{V_{ES}}$ lags $\boldsymbol{I_S}$ by 90° ($-Q_{ES}$).

Fig. 5 illustrates the electric vector diagrams of ES-1 in different operation modes with a resistive–inductive NCL. θ_Z is the load impedance angle. In the inductive mode, $\boldsymbol{V_{ES}}$ leads $\boldsymbol{I_S}$ by 90° and the NCL voltage vector $\boldsymbol{V_{NC}}$ is suppressed lower than $\boldsymbol{V_S}$. The NCL power is reduced to boost V_S to V_{S_ref}. While in the capacitive mode, $\boldsymbol{V_{ES}}$ lags $\boldsymbol{I_S}$ by 90° and $\boldsymbol{V_{NC}}$ is boosted higher than $\boldsymbol{V_S}$. The NCL power is increased to suppress V_S.

In the inductive mode, V_{NC} can be controlled to be substantially lower than V_S. In the capacitive mode, V_{NC} can be controlled to be slightly higher than V_S. Therefore, besides reactive power compensation, ES-1 has some active power compensation capability for balancing power supply and demand. However, its ability to reduce the active power of NCL is larger than that to increase it. In addition, the active power control and the reactive power control of the SL are coupled.

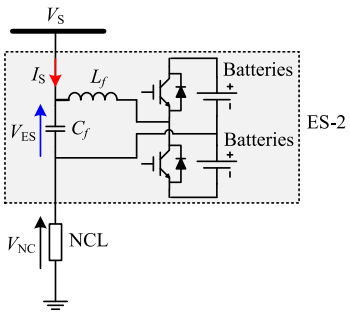

Fig. 6. Schematic of ES-2 with battery storage and an NCL.

ES-1 has the advantage of system simplicity and has been demonstrated as a fast DSM technique for mitigating voltage fluctuations [16], [19], [21] and both the voltage and frequency fluctuations in power grid [22]. Because the switching frequency of the power inverter of the ES is typically higher than 20 kHz, the bandwidth of the *LC* filter is typically one-tenth of the switching frequency. So the response of ES is very fast and is in the order of milliseconds. Wang *et al.* [23] confirm that ES-1 can be applied to resistive, capacitive, and inductive loads. Although original works of ES-1 were based on the single-phase version, three-phase ES-1 has been investigated for reducing unbalanced three-phase power system within a building [24]. Both the single-phase and three-phase ES-1 systems have been evaluated independently by Guangdong Power Company, Guangdong, China, with positive results [25]. The work of ES-1 in [26] and that of BTB ES in [17] shows that operating the adaptive ac mains within ±5% can ensure frequency stability.

B. Second ES With Battery Storage (ES-2)

The second generation of ES (ES-2) is reported in [27] to enhance the capability of ES. As shown in Fig. 6, its configuration is the same as that of ES-1 except that batteries are added to the dc link and act as energy storage components. The charging and discharging control circuits of batteries are omitted in the diagram. With batteries on the dc link, ES-2 can compensate the active and reactive power independently. The voltage vector of ES-2 is no longer limited to be perpendicular to its current vector. The operation of ES-2 is more flexible compared with ES-1. Besides inductive and capacitive reactive power, ES-2 can also provide positive or negative active power. In general, ES-2 has eight operation modes with different combinations of active power P_{ES} and reactive power Q_{ES}:

1) inductive power ($+jQ_{ES}$) compensation;
2) capacitive power ($-jQ_{ES}$) compensation;
3) positive real power ($+P_{ES}$) compensation;
4) negative real power ($-P_{ES}$) compensation;

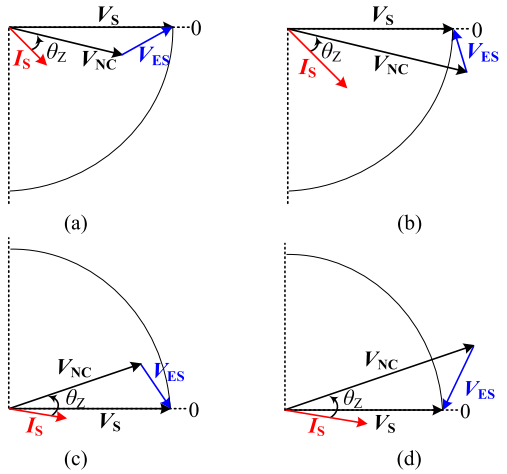

Fig. 7. Vector diagrams of ES-2 in different operation modes. (a) Inductive plus resistive ($+Q_{ES} \cdot +P_{ES}$) mode. (b) Inductive plus negative resistive ($+Q_{ES} \cdot -P_{ES}$) mode. (c) Capacitive plus resistive ($-Q_{ES} \cdot +P_{ES}$) mode. (d) Capacitive plus negative resistive ($-Q_{ES} \cdot -P_{ES}$) mode.

5) inductive and positive real power compensation ($+jQ_{ES} \cdot +P_{ES}$);
6) inductive and negative real power compensation ($+jQ_{ES} \cdot -P_{ES}$);
7) capacitive and positive real power compensation ($-jQ_{ES} \cdot +P_{ES}$);
8) capacitive and negative real power compensation ($-jQ_{ES} \cdot -P_{ES}$), where j refers to an imaginary number.

The vector diagrams of ES-2 in mode-5 to mode-8 are depicted in Fig. 7(a)–(d), respectively. The NCL is considered to be a resistive–inductive load. ES-2 expands its operating range into four quadrants with a phase difference between $\boldsymbol{V_{ES}}$ and $\boldsymbol{I_S}$. In Fig. 7(a) and (c) for resistive modes, $\boldsymbol{V_{ES}}$ leads or lags $\boldsymbol{I_S}$ less than 90° and $\boldsymbol{V_{NC}}$ is suppressed. ES-2 absorbs active power and batteries are charged. For the negative resistive modes in Fig. 7(b) and (d), $\boldsymbol{V_{ES}}$ leads or lags $\boldsymbol{I_S}$ more than 90° and $\boldsymbol{V_{NC}}$ is boosted. ES-2 generates active power and batteries are discharged. Compared with ES-1, even in the case of purely resistive NCL, the NCL power can be increased or decreased with the use of ES-2.

It is important to note that the suppression of $\boldsymbol{V_{NC}}$ does not necessarily result in the reduction of the total active power and the boost of $\boldsymbol{V_{NC}}$ does not ensure the increase in the total active power. For example, in Fig. 7(c) $\boldsymbol{V_{NC}}$ is suppressed and the active power of NCL is reduced. Meanwhile, ES-2 absorbs more active power than the power reduction of NCL. As a result, the total active power of the SL increases even though the power of NCL decreases. On the contrary, in Fig. 7(b) $\boldsymbol{V_{NC}}$ is boosted and the active power of NCL is increased. At the same time, ES-2 delivers more active power and some of the active power is fed back to the grid. So the total active power is reduced, while the NCL power of NCL increases.

Benefiting from the use of batteries, ES-2 can perform independent active and reactive power compensation in four quadrants. Both the NCL power and the total power depend on ES-2. Different from ES-1, the total active power and the reactive power of the load associated with ES-2 can be controlled independently. The additional flexibility of ES-2 is realized at the expense of the batteries and auxiliary circuits. However, if the distributed energy storage is considered as part of future smart grid strategy, the use of the distributed ES-2 will form a simple solution to cope with primary frequency control in the power grid. A research sponsored by the State Grid of China, Beijing, China [28] indicates that the distributed ES-2 can be used to optimize the operations in a distribution network such as reducing losses and achieving voltage regulation.

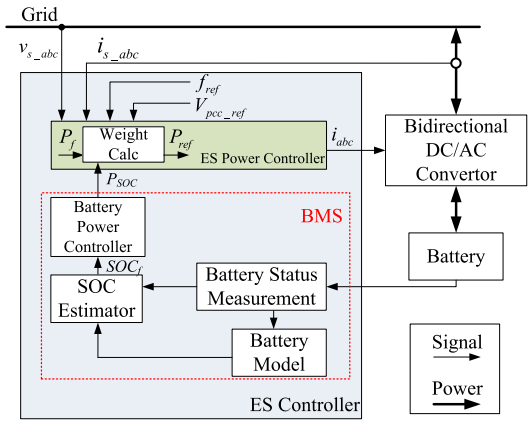

Fig. 8. Schematic of ES-3 with coordinated battery management control with the need for an NCL [29].

C. ES Based on Bidirectional Converter and Coordinated Battery Management Control (ES-3)

ES-2 can further be modified using a coordinated battery management scheme in association with a bidirectional ac/dc converter as shown in Fig. 8. Due to the limited capacity and the lifetime of a battery, it is necessary to consider the SOC variation so that the battery will not be overcharged or overdischarged. This third version of ES [29] has two distinct differences from ES-2. First, ES-3 does not need to work with NCL. Second, the SOC of the battery is set nominally at 0.5 so that the battery has the capacity to either absorb or release energy within a range of SOC that can preserve the battery life. Second-life batteries can be reused for this purpose.

In the control scheme, an instant SOC signal (SOC_f, which is normalized from 0 to 1) is introduced. An SOC reference of SOCref $= 0.5$ is set as a long-term target to maintain the battery at 50% SOC so that it is readily available to either absorb or deliver the active power for the power grid regulation purpose. There are two factors to determine the active power reference of ES-3, namely, P_f and P_{SOC}. P_f is a signal that controls the amount of active power delivered or adsorbed for the regulation of utility frequency, while P_{SOC} is a signal that controls the SOC of the battery storage system.

The actual active power reference signal P_{ref} is the weighted sum of these two signals. Hence

$$P_{\mathrm{ref}} = a P_{\mathrm{SOC}} + (1-a) P_f \tag{6}$$

where a is the weighted factor. The adaptive weighted factor a provides a way to coordinate between the battery management and the frequency regulation process, which is defined as a

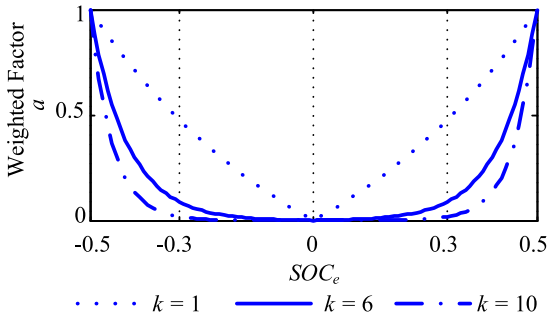

Fig. 9. Weighted factor a versus SOC_e with different values of k.

function depending on the absolute SOC error signal ($\mathrm{SOC}_e = \mathrm{SOC}_{\mathrm{ref}} - \mathrm{SOC}_f$, i.e., the deviation between the SOC reference and the instant SOC status). It can be expressed as

$$a = f(k, |\mathrm{SOC}_e|) = \frac{e^{2k|\mathrm{SOC}_e|} - e^{-k}}{1 - e^{-k}} \tag{7}$$

where k is a parameter which determines the profile of a as shown in Fig. 9. This function ensures that the charging and the discharging of the battery can be performed exponentially in a way that the charging/discharging rate is relatively faster when the absolute SOC error is large, while it is slower when the instant status of the SOC approaches the reference value $\mathrm{SOC}_{\mathrm{ref}}$. The choice of k depends on the configuration of the system and the design requirements. A higher value of k results in a wider range of the SOC error, as well as a more aggressive charging/discharging manner when the SOC is getting closer to the upper and lower limits of the working region. The proposed method not only provides an adaptively weighted priority between the mitigating of grid fluctuation and maintaining the storage system within the healthy SOC range but also avoids abrupt change in the output power for SOC control during transient operations. For ES-3, the SOC of the battery will be controlled gradually back to 0.5 after the stability of the mains voltage and/or frequency has been regained.

D. Back-to-Back ES

The BTB converter topology can be incorporated into the ES technology as the bidirectional dc–ac power converter to form the BTB ES [30], [31] in order not to use any battery in the dc voltage link. Fig. 10(a) shows the schematic of BTB ES. It consists of two PWM converters sharing a common dc voltage bus. One is a half-bridge converter with an *LC* filter. Its output is connected in series with NCL through an isolation transformer. The other is a half-bridge converter directly connected to the mains through an LCL filter. Fig. 10(b) shows the equivalent circuit of BTB ES which consists of a series ES and a shunt ES.

Compared with ES-2, BTB ES uses an additional shunt ES to replace the batteries on the dc link. The series ES operates in the same way as ES-2 and provides independent active and reactive power in four quadrants. Through changing the output of the series ES, the NCL power can be changed. The shunt

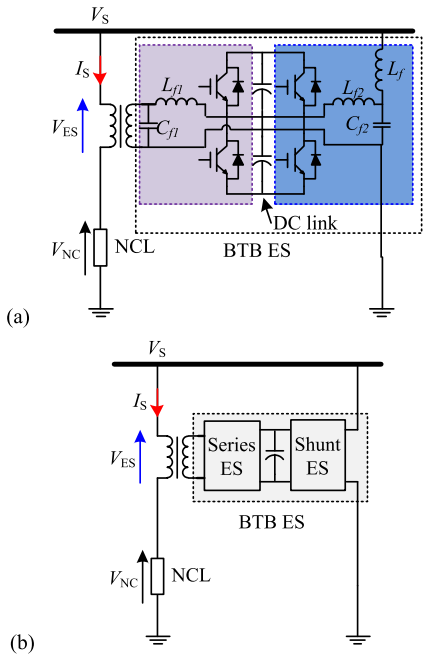

Fig. 10. Schematic of BTB ES. (a) Circuit diagram of BTB ES. (b) Equivalent circuit of BTB ES.

ES is used to balance the active power exchange between the series and shunt ES to maintain a constant dc voltage. Without the limitations of batteries, the operating range of BTB ES is greatly extended. An isolation transformer is necessary to decouple the output of the series and shunt converters of the original BTB-ES as shown in Fig. 10. However, a recent research article [32] confirms that the bidirectional power converter of the BTB-ES can be formed with a three-phase power inverter module without the need for an isolation transformer. This new circuit has a similar operating range to that of the original BTB-ES, but has the advantages of high compactness, low cost, and no transformer power loss.

E. Other ES Variants

1) PV-ES: In addition to the above four ESs, there are other ES variants. One ES variant integrating PV panel and PV-ES has been reported in [33] and [34]. Its schematic is shown in Fig. 11. Energy is harvested by the PV system, the dc output of which is connected across the dc-link capacitor of the dc voltage link of the ES. As pointed out in [27], the dc voltage source used in ES-2 allows decoupled active and reactive power control. The availability of the dc voltage source provided by the PV converter can play the same role and also allows the solar power flow through the PV converter. The concept of PV-ES is later generalized to link the ES with a range of renewable energy sources in [35].

2) Three-Phase ES: Three-phase ES has been explored for reducing power imbalance [24] and conduction loss of circulating current [36] in the three-phase power system of a building (Fig. 12). It is also used for extra functions such as active power filter in [37]. For distribution lines with relatively high resistance, a three-phase nine-switch matrix

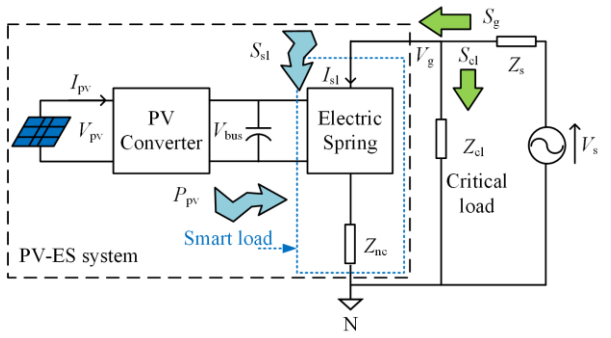

Fig. 11. Simplified schematic of a PV-ES system [33] (IEEE copyright).

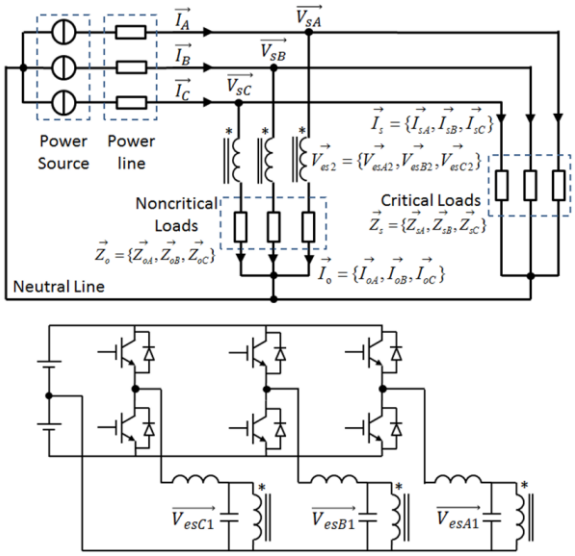

Fig. 12. Schematic of a three-phase ES-2 [24] (IEEE copyright).

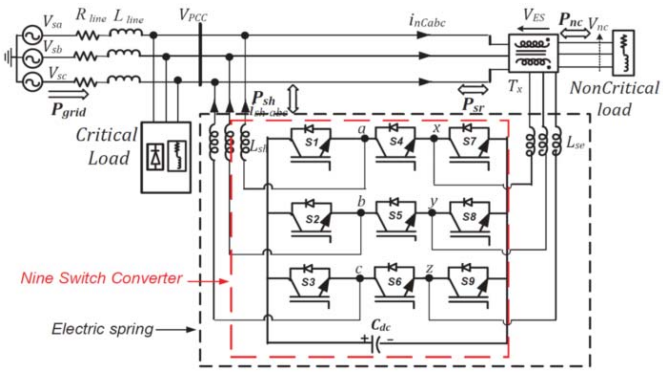

Fig. 13. Schematic of a three-phase E-1 based on a nine-switch matrix converter [38] (IEEE copyright).

power converter (Fig. 13) has been evaluated [38]. It allows the three-phase ES-1 to exchange bidirectional active power with the grid and perform the CL voltage compensation with a minimal magnitude of injected voltage. In addition, it relaxes the limitation of the quadrature relationship of the ES voltage and current.

The ES variants are derivatives of the four ESs (e.g., ES-1, ES-2, ES-3, and BTB ES) which demonstrate the basic structures of ESs. A comparison between the basic ES versions in terms of configuration, power controllability, and operating range is conducted and summarized in Table III. Generally speaking, the more components an ES has, the more flexibly it provides. ES-1 has the simplest configuration with the least components, while its power controllability and operating range are limited. Energy storage components like batteries enable ES-2 to operate flexibly with decoupled P & Q power control but increase the cost and weight. ES-3 works primarily with energy storage and can be independent of NCL, although its coordinated control with NCL power control can reduce the energy storage requirement. The trend of increasing acceptance of the distributed energy storage favors ES-2 and ES-3. BTB ES has the highest operating range without batteries. Its latest version can function without an isolation transformer [32]. While most of the ESs reported so far use voltage-source inverter, the use of a current-source inverter (CSI) is also a possibility [39].

TABLE III
COMPARISON OF ESS

ES versions and variants	No. of converters	Battery	Trans-former	Power con-trollability	Operating range
ES-1	1	No	No	Coupled	Smallest
ES-2	1	Yes	No	Independent	High
ES-3	1	Yes	No	Independent	High
BTB ES	2	Yes	No with new version [32]	Independent	Highest
PV-ES	1	No	No	Coupled	Medium
3-phase ES-2	3	Yes	Yes	Independent	High
Matrix Converter ES	1	No	Yes	Independent	High

It is important to note that the selection of ES topologies should depend on application requirements. ES-1 system is a good choice when space, weight, and cost are critical issues. The performance of the ES-2 system is comparable to the BTB ES system, while the power handling capacity of ES-2 is smaller than BTB ES. The transformer-less and lightweight design of ES-2 makes it compact and suitable for integration with PV panels. The BTB ES system is able to provide outstanding performance, while space and weight are not critical issues. The above information provides a basic guideline for engineers to design their ES systems according to different specifications.

F. Comparison Between ES and D-FACTS

Flexible AC transmission (FACTS) devices have been applied as power-electronic-based systems to improve the capability and stability of the power grid for at least two

TABLE IV
COMPARISON OF ES AND DYNAMIC VOLTAGE RESTORER (DVR)/D-STATCOM

Configuration	ES	DVR/D-STATCOM
Series	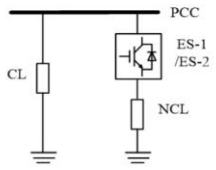	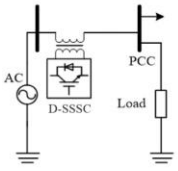
Shunt	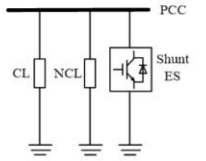	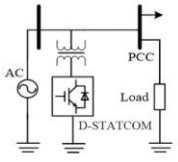
Series-Shunt	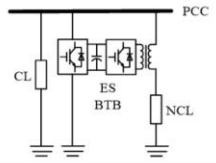	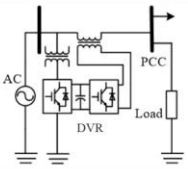

Note: DVR stands for dynamic voltage restorer.

decades. While both ES and FACTS devices are based on power converters, ES is different from FACTS at least in three aspects.

1) FACTS are typically installed on the transmission level in a centralized form, while ESs are deployed in the distributed network (although some FACTS can be installed on the distribution level as D-FACTS).
2) FACTS are controlled to regulate their "output" voltages at points of connection regardless of the input change. Each ES adopts "input" control to maintain the input voltage (i.e., the ac mains voltage) and let the output voltage fluctuate.
3) Most ESs are operated with NCL to form SLs. They work together to contribute the active and reactive power compensation. Even without battery on its dc link, ES-1 and BTB ES with NCL can still provide active power compensation. Table IV tabulates some differences between ES and D-FACTS.

A comparative case study conducted in [40] to control the voltage using ES and D-STATCOM reveals that a group of distributed ESs achieve better voltage regulation at various buses with significantly less total reactive power capacity than D-STATCOM. D-STATCOM can only tightly regulate the voltage at the point where it is installed. The effectiveness of the distributed ES also depends on the NCLs. The higher the portion of the NCL, the higher the ability for voltage control.

IV. CONTROL OF ES

The control methods applied for ES in the distributed network are generally classified into two types.

A. Control of Single ES

1) Basic Voltage Control: The initial ES (ES-1) is proposed to mitigate the voltage fluctuation caused by intermittent renewable source generation [16]. The basic voltage control diagram of ES-1 is illustrated in Fig. 14. To regulate the mains voltage, the voltage error between V_S and its reference V_{S_ref} is fed to a proportional–integral (PI) controller to produce the magnitude of the ES voltage $|V_{ES}|$. Meanwhile, to maintain a constant dc voltage, the dc voltage error is used to adjust the phase of the ES voltage θ_{ES} through another PI controller.

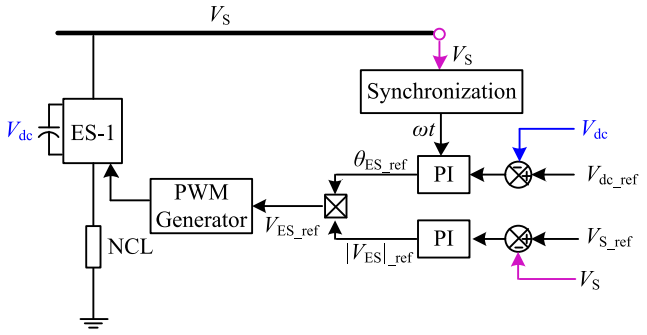

Fig. 14. Basic voltage control diagram for ES-1 [16].

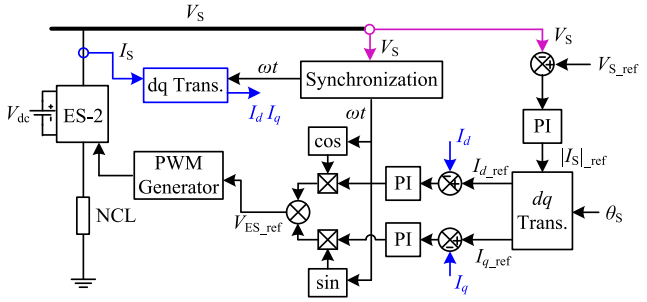

Fig. 15. *dq* control diagram for ES-2.

In practice, the ES voltage is not strictly perpendicular to its current because a small amount of active power should be consumed to meet the power loss of the ES converter. With obtained magnitude and phase information, one can get the desired ES voltage reference V_{ES_ref} and generate the PWM signal. This is a very simple method directly derived from the initial idea of ES-1 and easy to be implemented practically. Even $|V_{ES}|$ and θ_{ES} are controlled by two control loops, and they are inherently correlated. Each $|V_{ES}|$ has only one corresponding θ_{ES} and the active and reactive power are coupled together.

2) dq Control: For ES-2 with diversified operation modes, its controllability is also enhanced. A direct-quadrature (*dq*) control method can be used to decouple the active and reactive power control, which is based on the *dq* transformation as shown in (8) [41]. A sinusoidal quantity could be decomposed into direct and quadrature components. Taking $V_S\angle 0°$ as the synchronized direct axis reference, the current of the SL will be decomposed into active and reactive currents

$$\begin{cases} d = \dfrac{2}{T}\displaystyle\int_{T_n}^{T_{n+1}} A\sin(\omega t+\theta)\sin(\omega t)dt = A\cos\theta \\ q = \dfrac{2}{T}\displaystyle\int_{T_n}^{T_{n+1}} A\sin(\omega t+\theta)\cos(\omega t)dt = A\sin\theta. \end{cases} \tag{8}$$

A *dq* controller for ES-2 is illustrated in Fig. 15, which can regulate the mains voltage and control the power angle

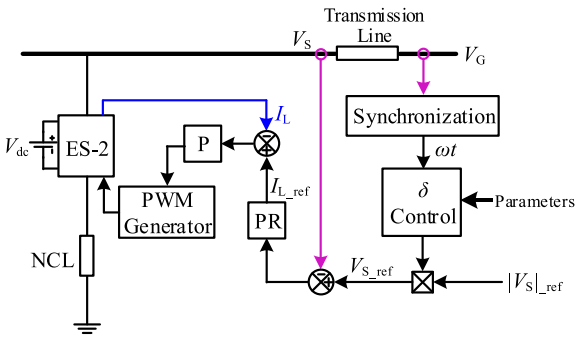

Fig. 16. δ control diagram for ES-2.

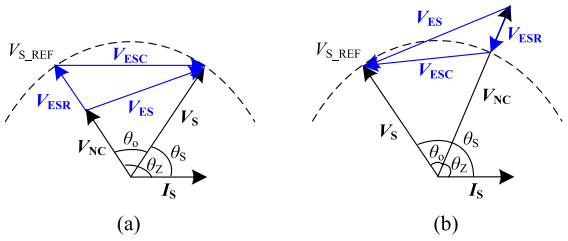

Fig. 17. Phasor diagram of RCD. (a) $\boldsymbol{V_{NC}}$ leading $\boldsymbol{V_S}$. (b) $\boldsymbol{V_{NC}}$ lagging V_S.

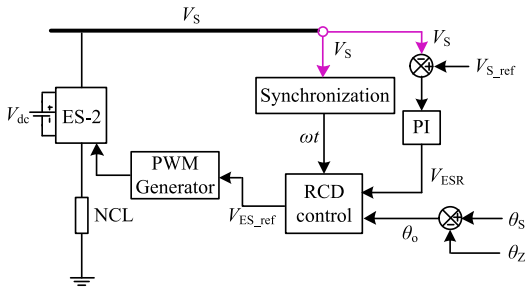

Fig. 18. RCD control diagram for ES-2.

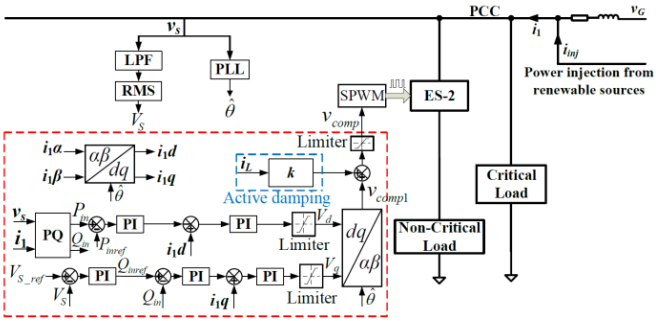

Fig. 19. Schematic of the modified SPD scheme [44] (IEEE copyright).

of the SL simultaneously. The mains voltage V_S is controlled by adjusting the current of the SL. With the desired power angle θ_S, both the reference current I_{S-ref} and the feedback current I_S are decomposed into d and q components and sent to independent d and q control loops to generate the ES voltage reference. This method decouples the active and reactive power control through dq transformation. It can be used for harmonics reduction and extended to BTB ES and three-phase ES as well. The disadvantage is that it uses three PI controllers and increases the control complexity.

3) δ Control: Fig. 16 shows the δ control for ES-2 to regulate the mains voltage by controlling the phase angle δ that local mains voltage lags the generator voltage [42]. With δ obtained through the δ control block, the local mains voltage reference V_{S_ref} is generated and sent to a PR controller to get the current reference I_{L_ref} for the inner current loop which controls the inductor current I_L of the ES converter.

With δ control, ES-2 takes different types of NCL into consideration and automatically determines its operation mode. However, the δ control block requires all the parameters of the system including the impedance of CL and NCL, the impedance of transmission line, the generator voltage, and the local mains voltage. Such information is usually unavailable in practice.

4) RCD Control: Another control scheme for ES-2 is called RCD control in which the ES voltage is decomposed into a radial component $\boldsymbol{V_{ESR}}$ and a chordal component $\boldsymbol{V_{ESC}}$ as shown in Fig. 17 [43]. Different $\boldsymbol{V_{ESR}}$ results in different load voltage $\boldsymbol{V_{NC}}$. Consequently, the current and apparent power of the SL change with $\boldsymbol{V_{ESR}}$. As for $\boldsymbol{V_{ESC}}$, it determines the power angle θ_o between the mains voltage $\boldsymbol{V_S}$ and the load voltage $\boldsymbol{V_{NC}}$. The power angle of the SL θ_S can be obtained using $\theta_S = \theta_o + \theta_Z$.

Fig. 18 depicts the RCD control scheme for ES-2. The mains voltage V_S is regulated by changing V_{ESR} through a PI controller. The power angle of the SL θ_S is controlled by changing the power angle θ_o. Then, the radial and chordal components of ES voltage can be obtained through the RCD control block. The RCD control decouples voltage and power angle control and greatly simplifies the control. Compared with dq control, only one PI controller is needed when the load impedance angle θ_Z is known.

5) Modified Simple Power Decoupling (SPD) Method: The initial SPD method [43] has several limitations that key members of the same research group published a modified SPD method in [44]. The modified SPD control scheme is designed without needing the values of circuit parameters and simultaneously offering a faster transient response over the original SPD scheme. It is achieved using two current loops that regulate the line current drawn by the load on the d-axis and q-axis separately as shown in Fig. 19. An active damping control is needed in this scheme. Despite that the circuit parameter values are not needed, this modified SPD method requires the ES output current in the control scheme to achieve a damped response. Wang *et al.* [44] stress that this control cannot work effectively without the ES output current information.

B. Control of a Group of Distributed ESs

All control methods described previously are applied to a single ES. The contribution of a single ES is limited due to its limited power capacity. Similar to the array of mechanical springs under a mattress, a large group of distributed ESs can be installed in the distribution network for providing robust stability support to the power grid. For now, there are

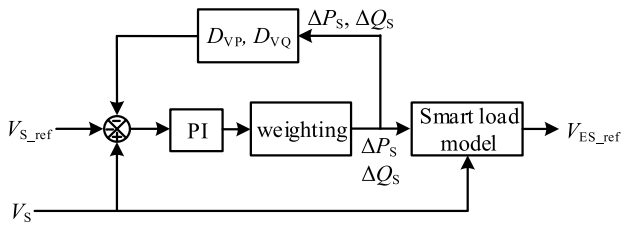

Fig. 20. Droop control for the distributed SL using ES.

two types of control methods introduced for distributed ES to enhance their effectiveness, namely, droop control and consensus control.

1) Droop Control: Droop control is widely used for cooperation of traditional power generators [45], [46]. The droop concept is first applied to multiples ES-1 in [47] for voltage control and it prevents competition among ESs at the same time. The mains voltage reference V_{Sx_ref} for the ES installed at the distance x is automatically adjusted by a droop constant so that the ES far away from generation will not be overload.

Another droop control method for BTB ES is proposed for voltage control in [48]. As shown in Fig. 20, the mains voltage references for all ESs are the same, but the voltage error is updated by the active and reactive power change in SL. Droop gains D_{VP} and D_{VQ} are designed to share the droop effect between the active and reactive power. Updated voltage error is fed to a PI controller and weighted to derive the required active and reactive power change in the SL (ΔP_S, ΔQ_S). Then the SL model can be used to calculate the required ES voltage. This idea can also be applied to frequency regulation [49] in which only one droop gain (D) is used to update the frequency with the active power change in SL.

Droop control modulates the nominal value of the voltage reference (e.g., 1.0 pu) to share the burden and thus ensures that ESs do not fight against each other. However, droop gains are highly dependent on the R/X ratio of the network and the location of ES. Therefore, it is difficult to tune the droop gains. Good cooperation and work-sharing are barely acceptable without reasonable droop gains and control structure.

2) Consensus Control: The consensus algorithm is also commonly used for multiagent systems and has been introduced to control generators, plug-in EVs, and energy storage systems in the power grid [50]– [52]. It is applied to multiple ESs and practically verified for the first time in [53]. The basic idea is each ES behaves as an agent and shares its local information state with the neighboring ES agents. Through an appropriate algorithm, each ES acts to update its information state so that the information states of all the ESs converge to a consensus. In Fig. 21, the local information is the reactive power Q_{ES} of each ES. There are three ESs in the network, and they share the information of Q_{ES}/Q_{ES_MAX} with their neighbors. The consensus algorithm is designed to regulate the mains voltage with equal reactive power-sharing which generates a compensation adjustment value to the primary voltage set point.

Consensus control is also introduced to enable distributed ES to achieve voltage and frequency regulation with sharing

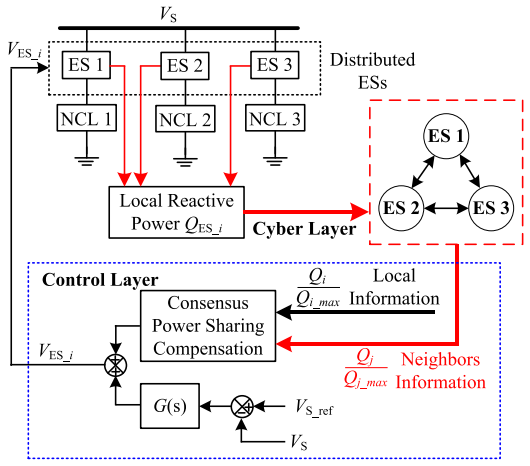

Fig. 21. Consensus control of the distributed ES for voltage regulation.

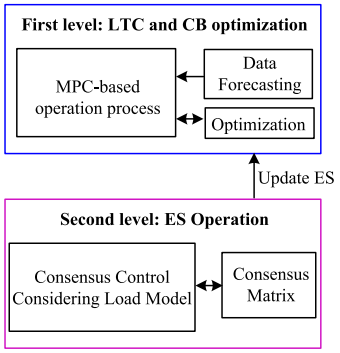

Fig. 22. Two-level voltage control scheme using ES.

active and reactive power, respectively, in [22]. Compared with droop control, consensus control can accurately control the responsibility of each ES. These two methods are complementary and used together for voltage control. Fig. 22 shows that a two-level voltage control scheme is developed to optimize the critical bus voltage at chosen locations [54]. The upper level adopts a model predictive control (MPC)-based method to determine the optimal cooperation of load tap changer (LTC) and capacitor banks (CBs). Then, in the lower level, the critical bus voltage is regulated through responsibility-sharing among ESs through consensus control. In case of communication failure, either the droop control or the top-level control could act as a safety guard to ensure safe operation.

The outstanding feature of consensus control is that responsibility-sharing with high consistency can be implemented. However, local communication is necessary for consensus control. The time delay and coupling strength between the neighboring agents need careful consideration to ensure stability and satisfactory convergence rate, especially when the number of agents increases. Recently, the droop control and consensus control are practically implemented in real-time in a distributed ES system [55]. When the cyber layer is in normal condition, consensus control takes actions for the distributed ES to provide voltage and frequency stability. When the cyber layer is attacked or not available, the control will be reverted to droop control.

TABLE V
SUMMARY OF CONTROL METHODS FOR ES

Category	Control method	Application	Features
Single ES	Basic voltage control	ES-1 Matrix Converter ES	Simple PQ Coupled
	dq control	ES-2 BTB ES 3-phase ES-2	PQ decoupled
	δ control	ES-2	Difficult implementation
	RCD control	ES-2 PV-ES	PQ coupled
	Modified SDP	ES-2	PQ decoupled
Distributed ES	Droop control	All ES	Droop gain No communication
	Consensus control	All ES	Responsibility sharing Local communication

*PQ-Active and reactive power

All the control methods for ES are classified into two categories and are summarized in Table V. Basic voltage control, *dq* control, δ control, RCD control, and modified SPD control are developed to control single ES, while droop control and consensus control are designed to coordinate a group of distributed ESs.

V. DCESs IN DC MICROGRIDS

The proliferation of the information and communication technology (ICT), EVs, and energy storages has led to the growing use of dc appliances. This makes the dc microgrids increasingly feasible in delivering cost-efficient electricity than its ac counterparts. Meanwhile, the industries are replacing their energy sources with renewables for reducing the greenhouse gas emission so as to alleviate the global warming issue. Multinational corporations such as Facebook, Microsoft, Apple, and Google have committed to achieve "100% renewables" in their global operations of data centers, cloud services, manufacture, and so on. Spurred by growing interest on the migration of ac power systems to dc power systems, the DCES was proposed as a means to tackle the possible instability issues of the dc power systems and microgrids, in relation to the use of more intermittent renewable resources. With respect to the recent research findings on DCES, the physical operating principles, hardware circuit topologies, control, and applications of the DCES will be summarized in this section.

A. Series and Shunt DCES

A typical unipolar dc grid integrated with the DCES is depicted as shown in Fig. 23. Under such a configuration, the supply–demand power imbalance, the relatively long-distance (LV) power delivery through distribution lines, the possible occasional faults (e.g., faults F_L and F_U in Fig. 22), and the integration of appliances with harmonic

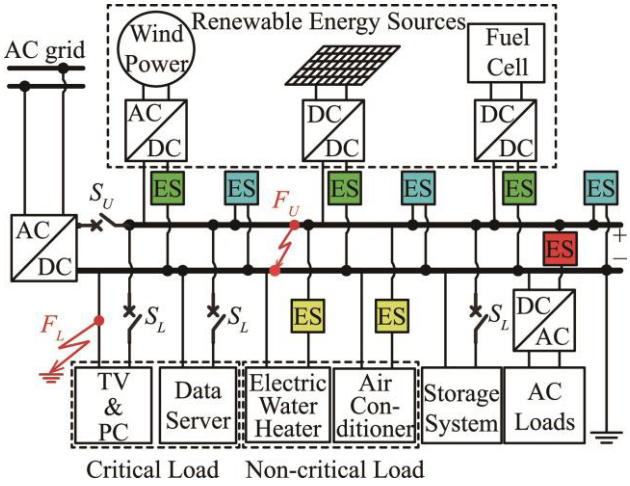

Fig. 23. DCES-integrated unipolar dc grid.

pollution sources (e.g., single-phase ac–dc conversion) to the dc grid can potentially render the voltage instability issues of 1) dc voltage variation; 2) voltage droop; 3) voltage flicker; and 4) harmonic voltage, of which the corresponding waveforms are illustrated as shown in Fig. 24. Irrespective of its hardware circuit topology, the DCES is essentially a decentralized DSM unit, which is massively scattered in dc power systems, such as that shown in Fig. 23 for addressing the aforementioned instability issues in a distributed manner [56].

The DCES can be categorized into series and shunt types. The basic configuration of the series type DCES in a dc grid is shown in Fig. 25. In terms of circuitry, it is a controllable bipolar voltage source which is connected in series with an NCL. Similar to the ac counterpart, such a configuration enables an SL branch. The active attenuation of the SL power can be achieved by adjusting the voltage of DCES. The power quality of the CLs can be guaranteed with the SL compensating these voltage instability issues. The general operating principles of the series-type DCES is first reported in [56], in which the steady-state operating modes of the series-type DCES associated with 1) positive constant-resistive loads; 2) negative constant-resistive loads; 3) positive constant-power loads; and 4) negative constant-power loads have been analyzed, respectively.

In the event that the appliances of dc microgrids are generally critical, that is, few NCLs can be connected to the series-type DCES, the shunt-type DCES can be alternatively used for the bus voltage regulation. The basic circuit model of a shunt-type DCES incorporated to the dc grid is illustrated in Fig. 26. The shunt-type DCES is essentially a controllable bidirectional current source. It is directly connected to the dc bus and does not associate with any NCL [57]. In [57], a systematic comparative study is performed between the series- and shunt-type DCES. With respect to different applications, the advantages and disadvantages of both types of DCES are summarized as shown in Table VI.

B. Hardware Topology of DCES

In the reported research works [56] and [57], the half- and full-bridge dc–dc converters are applied to achieve the

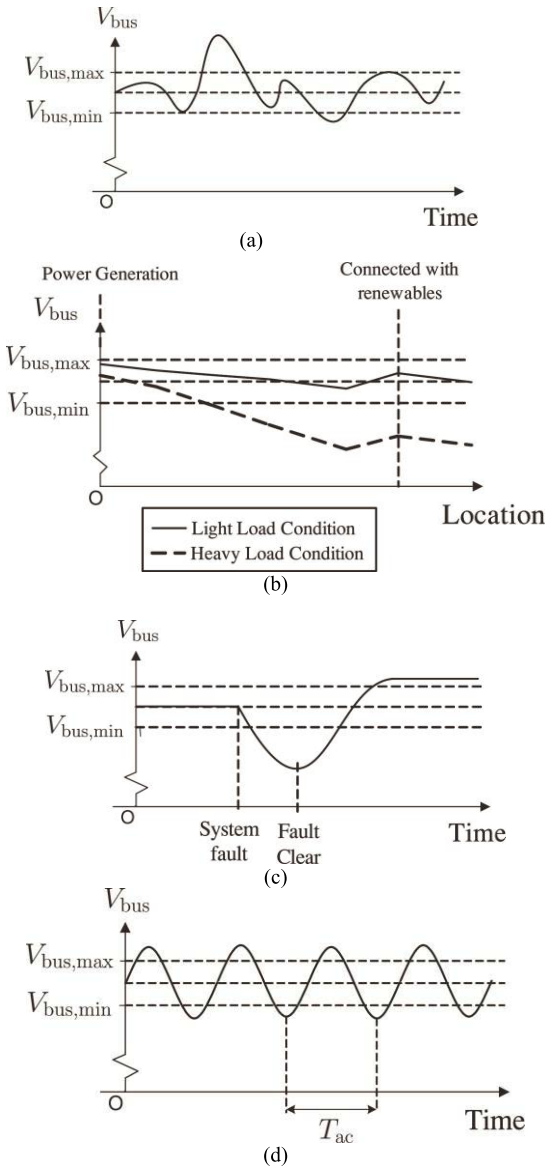

Fig. 24. Different voltage issues in the dc power systems. (a) DC voltage variation. (b) Droop effect. (c) Voltage flicker. (d) Harmonic voltage.

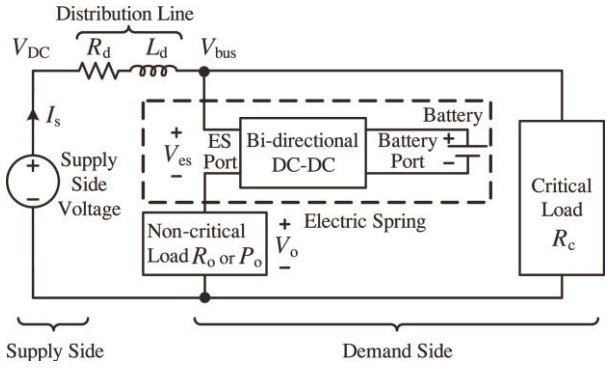

Fig. 25. Basic configuration of the series-type DCES.

DCES functions. These conventional circuit topologies provide a coupled relationship between the harmonic power and the dc power of the DCES batteries in the concurrent operations

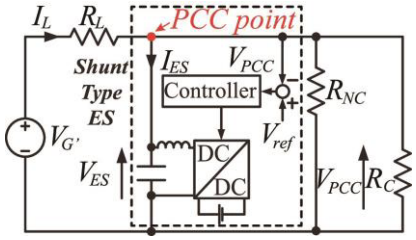

Fig. 26. Basic configuration of the shunt-type DCES.

TABLE VI
COMPARISON OF SERIES- AND SHUNT-TYPE DCES

	Series Type	Shunt Type
Dynamic response	× Slow × NCL-dependent	√ Fast
Supply-demand balancing	√ Real-time load manipulation √ Storage reduction	× Incapable of load manipulation
Harmonic cancellation	× Power consuming × NCL-dependent	√ Consume little power
Providing fault-ride-through support	× Slow × Affect NCL	√ Fast

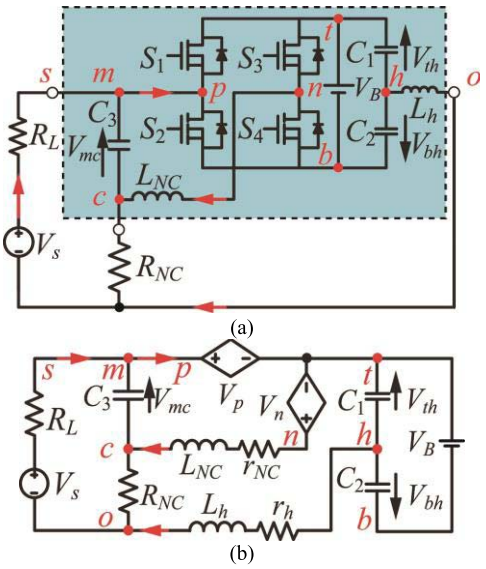

Fig. 27. Schematics of (a) H-DCES and (b) corresponding equivalent circuit.

of supply–demand balancing and harmonic cancellation. This can lead to a low energy efficiency and a short lifetime of the batteries. In [58], an H-DCES, which is essentially a dc-split full-bridge dc–dc converter, is proposed to address this issue.

The schematic diagrams of the H-DCES and the corresponding equivalent circuit are shown in Fig. 27. Compared with the series-type (Fig. 24) and shunt-type (Fig. 25) ES, the H-DCES has a split dc-link capacitor branch, which bypasses the dc-link batteries and the NCL from the harmonic current path. The harmonic power and dc power can be stored in split dc-link capacitors and batteries, separately.

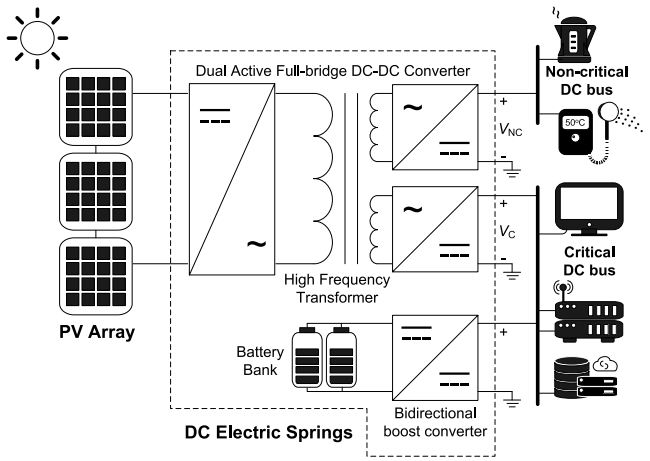

Fig. 28. Schematic of a three-port DCES system [59] (copyright IET).

Besides this nonisolated topology of H-DCES for achieving the decoupling of the harmonic and dc powers, a three-port isolated topology of DCES (Fig. 28) has been reported in [59] for isolating the dc power supply, NCL, and CL. The circuit topology comprises a three-port isolated dual-active full-bridge dc–dc converter and a bidirectional boost converter (BBC). The dc power supply, NCL, and CL are connected to the three ports, respectively. The batteries are connected to the CL through the BBC. Essentially, the NCL is operated to consume the disruptive part of the renewable dc power supply, while the batteries are controlled to compensate the power imbalance between the loads and the dc power supply. Although the power flows of NCL, CL, and dc power supply can be independently controlled in this topology, it involves the use of considerable power electronics, that is, 14 active switches and a high-frequency three-port transformer.

C. Control and Application of Multiple DCESs

The schematic diagrams of a dc distribution grid and a series-type DCES integrated dc microgrid are shown in Fig. 29(a) and (b), respectively. To achieve the cooperative and optimum operation of the dc power grid, the centralized, decentralized, and distributed control methods can be applied to various DCESs in the system.

In [60], a centralized MPC scheme is proposed to operate the series-type DCES in dc distribution grids. In this work, a dual-objective cost function is formulated to minimize the nodal bus voltage deviation and the distribution line loss. In the prediction of the optimum bus voltage references, the nodal voltages are discretized for enabling an enumerative evaluation of the penalty cost. Then, the series-type DCES will be operated by the local voltage controller to regulate the nodal voltage according to the calculated voltage reference. Although this centralized method can achieve a reasonably guaranteed global optimal condition, it demands synchronized measurements, real-time data communication, and a significant amount of computation. Considering the cost of the communication infrastructure, this method may be more suitable for small distribution systems rather than large ones.

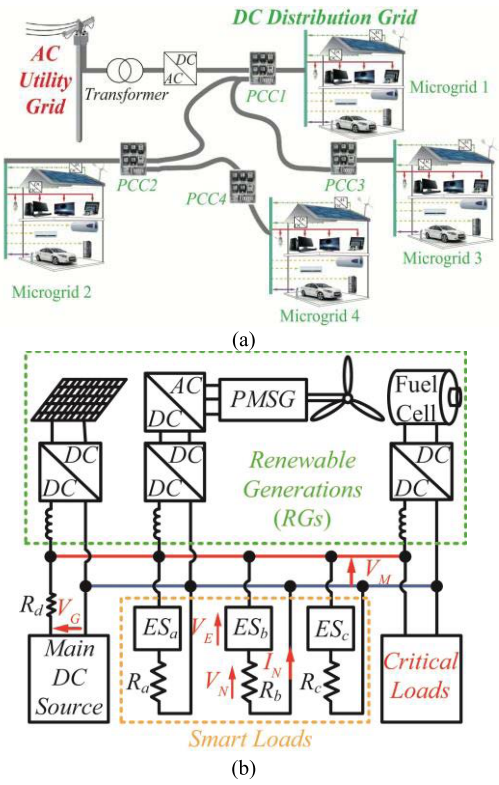

Fig. 29. Illustration of (a) dc distribution grid and (b) dc microgrid integrated with multiple series-type DCES [61].

To regulate the bus voltage against the intermittent renewable generation with reduced storage capacity, a decentralized droop control scheme is proposed in [61] for coordinating the operation of multiple series-type DCES in dc microgrids. The investigated system topology is shown in Fig. 29(b). In this work, the SL branches share a common dc bus. The proposed droop control scheme can operate the series-type DCES to achieve the minimum charging and discharging power to cope with the voltage sag and overvoltage, respectively. In this way, the overall energy deviation of the DCES batteries, as well as the required storage capacity, can be reduced. This method is practical and independent of the communication network. However, it cannot eliminate the dc bus voltage deviation. The line impedance between different series-type DCESs will affect the performance of the controller.

In [62] and [63], a distributed cooperative control scheme is applied on the three-port DCES [59] and the shunt-type DCES to achieve the unanimous regulation of bus voltages and battery SOC. This control scheme consists of a primary droop controller and a secondary consensus controller. With local and neighboring measurements, this control scheme eliminates the impact of line impedance on the load-sharing of DCES and the bus voltage regulation. Thus, it has a better voltage regulation than the conventional droop control scheme and a lower requirement on the communication system than the centralized control scheme, which makes it suitable for implementation in large power systems.

Besides the applications of DCES in unipolar dc grids, the unbalanced voltage suppression of the DCES in bipolar dc distribution grids is reported in [64]. In the work,

the coupled relationship between the positive-pole and negative-pole voltages is mathematically derived and it is demonstrated that the investigated DCES-integrated bipolar dc grid is a coupled two-input-two-output system. To enhance the dynamic performance of the system in restoring the respective pole voltages and reducing the neutral current, the decoupling control variables are introduced and fed forward to eliminate the coupling between the two control inputs. With this decoupling control method, the original two-input-two-output system is transformed into two independent single-input-single-output systems.

VI. System-Level Impact

A precursor to studying the system-level impact of ES is to develop its dynamic model which is compatible with large-scale power system simulation model. Modeling of ES for power system studies is discussed first in this section followed by its effectiveness toward voltage regulation, frequency control, power quality improvement, system restoration, and impact on stability.

A. Modeling of ES for System Studies

A dynamic simulation model of ES appropriate for voltage and frequency control studies at the power system level is reported in [65]. The case studies show a close match between the simulation and experimental results confirming the accuracy of the proposed model. Slight discrepancies are attributed to the absence of the dc-link voltage control loop which, if included, will drastically slow down the simulation with little improvement in accuracy. In [66], a dynamic and modular ES model is presented that can incorporate the controller design and the dynamics of the power electronic circuits. The experimental results are used to reduce the order of this dynamic model to suit both the circuit and system simulations. The modular approach allows the circuit and controller of the ES model and the load module to be combined in the d–q frame. The performance of the ES model is validated on the IEEE 13-node power system and a microgrid.

A linearized state-space model of the distribution network with multiple ES-1s with vector control is developed in [67] which is extendible to include inverter-interfaced distributed generations (DGs), energy storage, active loads, and so on. The state-space model is used to analyze the impact of distance of an ES from the substation, the proximity between the adjacent ESs, and the R/X ratio of the network on small-signal stability and compared against the case with equivalent DG inverters. This state-space model of vector-controlled ES-1 could be incorporated into the stability models of microgrids to study how droop control of ES impacts the overall stability.

B. Voltage Regulation

1) Distribution Network: The effectiveness of the distributed voltage control using ES is compared against the traditional single-point control with STATCOM in [40]. A case study on a part of the distribution network in Sha Lo Wan Bay in Hong Kong shows that a group of ESs achieve better

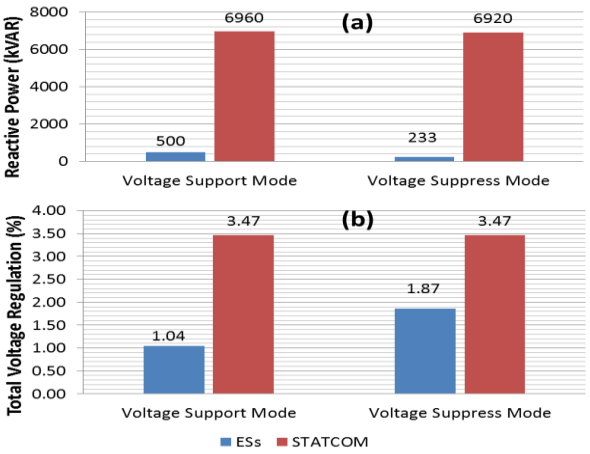

Fig. 30. (a) Reactive power required and (b) total voltage regulation achieved collectively by all the distributed ESs and the STATCOM under voltage support and suppress condition for the Sha Lo Wan Bay case study in [40].

total voltage regulation than STATCOM with less overall reactive power capacity as shown in Fig. 30. In [48], SLs with BTB ES are shown to mitigate voltage problems caused by PV generation and EV charging in LV distribution networks more effectively than ES-1 especially, under the overvoltage condition. Yang *et al.* [33] report the use of ES to maximize PV power and simultaneously ensure supply–demand balance obviating (or reducing) the need for battery storage. In [30], the effectiveness of BTB ES in suppressing the mains voltage compared with ES-1 is demonstrated with a weak power system.

A specific situation of overvoltage prevention using ES with storage-type EWHs is considered in [68]. A case study on the Sha Lo Bay residential LV network in Lantau Island, Hong Kong, demonstrates the effectiveness of the proposed approach in absorbing excess PV power to prevent overvoltage. In [69], BTB ES in the output voltage control mode is used to tackle under- and overvoltage problems enabling larger PV and EV penetration. Both load- and feeder-level approaches are effective in accommodating PV generation and EV charging, but the former requires overall higher converter capacity than the latter and produces better voltage regulation at the load terminals with larger demand response provision. Moreover, higher PV throughput is achieved with load-level ES despite higher losses in the feeder and the ES itself, but the feeder-side voltage could exceed the stipulated upper limit.

In [54], a two-level voltage management scheme with LTC and CBs at the upper level and ES at the lower level is demonstrated using consensus control allowing different voltage regulation devices to work together to maintain the voltage of critical buses by sharing the responsibility. Zheng *et al.* [70] also use a consensus algorithm to coordinate multiple ESs for maintaining critical bus voltage in distribution systems with ultrahigh renewable penetration. This yields similar voltage suppression capability as the conventional ES but better voltage support with the ESs sharing the burden using limited communication.

A risk-limiting approach to the ES planning method is reported in [71] to obtain the optimal ES configuration (number, locations, capacities, and types) to mitigate the voltage violations considering the uncertainties in renewable generation. An optimal voltage control method for an active distribution network with ES is presented in [72]. The critical bus voltage is regulated with minimum ES voltage is a distributed but coordinated fashion for which the load parameters are estimated in real-time using nonintrusive load monitoring. A decoupled dual functionality of ES is demonstrated in [34] by combining feeder voltage regulation and injection of roof-top PV power with drastic changes in solar irradiance. In [73], the performance of ES is evaluated operationally and economically using a backward/forward sweep method for optimal power flow and the real price and load data of the ISO-NE market. The results of the case study confirm that the ES improves power loss, voltage profile, power factor, and stability, while it reduces the operation cost. In [74], a hybrid method for ES control combining the data-driven and analytical models is demonstrated for voltage control in the IEEE 15-node distribution network. Three data-driven models based on the extreme learning machine are built which are shown to be more accurate than the analytical model in predicting the system states.

2) AC Microgrid: In [75], ESs in conjunction with the water heating system as NCLs are used to regulate the CL voltages in an islanded microgrid with intermittent renewables. The temperature constraint of the water heating system and the ramping constraint of a diesel generator are managed using the MPC. SLs having the ES in series with the CL are considered in [76] to mitigate voltage fluctuations in low-inertia nanogrids. This is shown to reduce the burden on energy storage depending on the percentage of the loads that are converted into SLs. In [77], several interconnected microgrids with ES are shown to form a transactive energy system. An optimization model and the solution method are presented to determine the optimal operating points for multiple ESs in the microgrid to minimize the total voltage deviation.

A hybrid ES integrated with renewable generation and NCL is used in [35] power control and reduction of battery storage capacity in ac microgrids. This achieves an extended operating region for power control compared with the conventional way of using battery storage and ES. Moreover, the hybrid ES prevents overcharge and overdischarge of the battery by limiting its SOC within a predetermined critical region to preserve the lifetime.

Overall, BTB ES has been found to be the most flexible and effective for voltage regulation in the ac distribution network and microgrids, in general, unless specific situations such as PV or EV integration and/or the need for distributed energy storage favor other ES types. This is true irrespective of whether a distinction is made between critical and NCLs. By complementing the voltage support, the ES can not only reduce the need for battery storage but also improve the management of the batteries to extend their lifetime. Use of distributed control with minimal reliance on communication is crucial for voltage regulation with ES.

3) DC Microgrid: Regulation of dc microgrid bus voltage using DCES is demonstrated in [57]. Both the series- and shunt-connected DCES are considered for dc bus voltage regulation, double-line frequency harmonic compensation, and fault-ride-through support. Faster dynamic response capability of the shunt ES is used for fault-ride-through (FRT) support to tackle the stability problem in dc microgrids with intermittent renewable energy sources. In [60], MPC with both the adaptive and nonadaptive weighting factors is used to coordinate multiple DCESs to regulate the dc bus voltage and reduce the power loss on the distribution lines. Use of MPC with adaptive weighting factor results in less power loss than the nonadaptive version. A 48-V 5-bus dc microgrid experimental setup is used to validate dc bus voltage regulation in the above two references.

A distributed cooperative control is used in [63] for multiple DCESs with dc/dc three-port converter, bidirectional buck–boost converter, and battery. Allocation of the primary and secondary control duty among multiple DCESs is exercised using droop and consensus, respectively, while balancing the SOC of the batteries associated with the DCESs. In [68], an energy management system (EMS) for the above DCES is presented which controls the operating mode transition of the buck–boost converter, changes the operating status of the battery, and realizes multiple charging and/or discharging mechanism. Thus, the EMS can regulate the voltage of the dc microgrid and also maintain the SOC of the battery within a reasonable range to extend the battery life.

C. Frequency Control

1) Primary Frequency Control: In [49], the effectiveness of the SLs with ES-1 in improving mains frequency regulation with a little relaxation in mains voltage tolerance is demonstrated through a case study on the IEEE 37-bus test distribution network. Sensitivity analysis is included to show the effectiveness and limitations of SLs for varying load power factors, the proportion of SLs, and system strengths. To achieve primary frequency control with ES-1, the mains voltage regulation is compromised slightly (still staying well within the acceptable limits) which can be overcome with BTB ES. A control strategy based on the relationship between the active power of NCL and the voltage of CL is used in [26] to show that the ES can stabilize frequency fluctuations.

Liu *et al.* [78] study both the automatic generation control and the load-side control using a switched distributed controller designed for each load bus in a transmission network. Selection of control gains and design of the switching signal and the communication network for the load-side controller is discussed. The local stability criterion of the system with the proposed controller is established using linearization techniques. The effectiveness of the proposed controller for grid frequency control is demonstrated using the modified WSCC 9-bus test system with a single control area and the IEEE 39-bus test system with two control areas.

The concept of ES aggregators is used in [79] to achieve the required coordinated active power response to regulate grid frequency and maintain the bus voltages within the acceptable limits. A distributed leader-following consensus

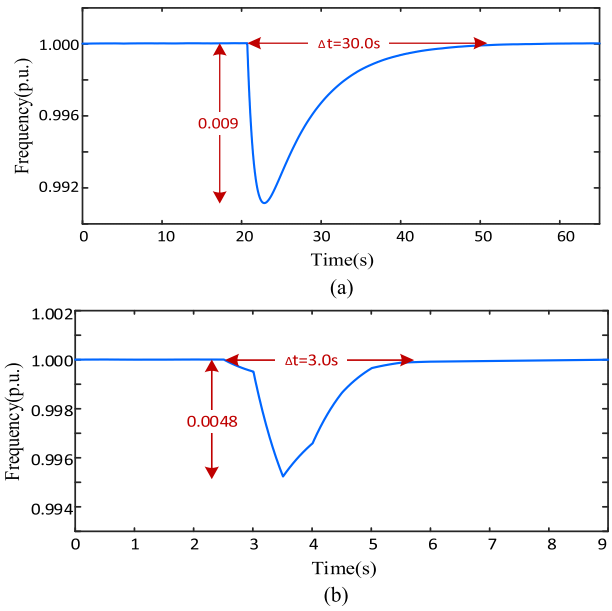

Fig. 31. Frequency of a microgrid after a 20% load change (a) without and (b) with the use of distributed ES [55].

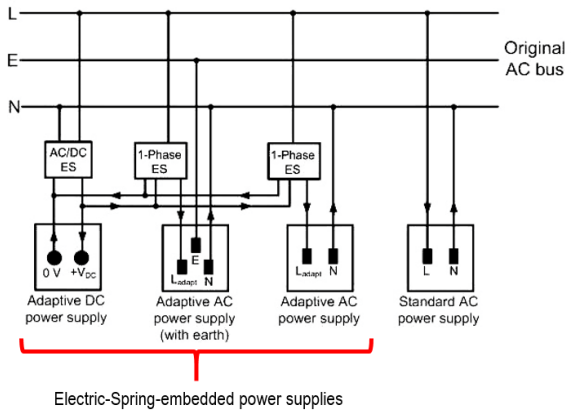

Fig. 32. Schematic of an ES-embedded power supply infrastructure.

algorithm is adopted for ES aggregators to obtain the updated active power set points and achieve the required active power response in a coordinated way. The simulation results show that ES aggregators can cooperatively provide the required active power response in time and regulate the frequency more effectively than the traditional automatic generation control while keeping the bus voltages within the admissible range.

2) Frequency Control in Isolated Microgrids: An ES with a bidirectional grid-connected power converter with a battery bank is used in [29] to reduce both the voltage and frequency fluctuations in an isolated microgrid. A modified dead zone control circuit with a hysteresis band embedded on the existing active–reactive power decoupling control scheme for ES is used. Both the simulation and experimental results are presented to illustrate the monitoring, charging/discharging management, and output power control. In [55], consensus control with a circular communication link at the cyber layer is used for a cluster of ESs to provide local voltage and system frequency regulations in a microgrid. Droop control (without communication) and consensus control (with the communication) are shown to be complementary. The latter achieves better power-sharing with local communication but can revert to droop control when local communication is not available. Fig. 31 shows the practical measurements of the grid frequency after a sudden load increase of 20% with and without the use of distributed ES. It can be observed that the ES can quickly restore the grid frequency of the microgrid after the load disturbance.

D. Demand Response Through Point-of-Load Voltage Control

The most common way to exploit the voltage dependence of loads for peak demand reduction is by decreasing the operating voltage of the distribution feeders, known as the conservation voltage reduction (CVR) [80], [81]. In practice, this is usually done through transformers at the primary substation, but equivalent power electronic solutions such as a "Smart Transformer" [82] at the secondary substation and mid-feeder compensation [69] have been reported as well. They are effective as long as there is sufficient room to maneuver the voltage without violating the stipulated voltage limits at the far end of the feeders. However, during high loading and/or nonuniform loading across parallel feeders, the available margin for changing the voltage from the substation (or at some point on the feeder) could be very limited necessitating distributed point-of-load voltage control through ES.

The collective contribution of both the static- and motor-type SLs to aggregated demand response provision is demonstrated in [31] through a case study on the Great Britain (GB) transmission system. The study shows that the SLs collectively offer a short-term power reserve which is comparable to the spinning reserve in the GB system, and thus can ensure acceptable frequency deviation and its rate of change following a large infeed loss. Guo *et al.* [17] quantify the aggregate demand reduction through distributed voltage control at the supply point of a cluster of domestic customers. This is shown to be more effective than voltage control at substations (VCS) especially, under high loading. A high-resolution stochastic demand model and the aggregate power-voltage sensitivity of individual domestic customers are used for the study. The rating of the voltage compensators required for polyvinyl chloride (PVC) is evaluated to weigh the benefits against the required investment. Virtual inertia contribution through fast demand response capability of PVC using ES is quantified in [83]. For the first time, this article has shown that the demand side could play a significant role in complementing the depleting inertial contribution from the supply side which has inherent limitations as well. For instance, the virtual inertia contribution from wind turbines is limited by the recovery phase (depending on the prevailing wind speed), the rated capacity of the grid interface power converters, the mechanical stress on the turbine components, and the associated impact on lifetime. For solar PV, virtual inertia can be provided by operating below the maximum available power (i.e., part-rated operation) which could be expensive. This is where SLs could

complement the existing solutions as an additional source of virtual inertia.

The available demand response capability through point-of-load voltage control would vary with the time of the day depending on the incidence of different types of voltage-dependent loads and also the voltage profile across the feeders. It is important for the grid operators to know the aggregate power reserve from the voltage-dependent loads during different times of the day to schedule other forms of reserves accordingly. Chakravorty *et al.* [84] present such a methodology to estimate such power reserve from the measured power and voltage at the bulk supply points without knowing the actual distribution network topology and/or load profile of individual customers. This is applied to estimate the time variation in the aggregate reserve offered by the voltage-dependent loads within the domestic sector in GB.

Fast response time of ES enables them to collectively contribute to frequency control over a range of timescales from inertial to fast frequency response (<1 s) to primary frequency regulation (<10 s). Similar to the case of voltage regulation, the ES can effectively complement energy storage for frequency control. However, the challenge is to provide accurate system-wide quantification of the aggregate response capability of the ES/SL which the system operators can rely on whenever it is necessary.

E. Harmonics Reduction

The effectiveness of ES-2 for harmonic reduction and power factor correction is demonstrated experimentally on a small-scale power grid in [41]. Coordinated operation of ES-2 for harmonics reduction and power factor correction and ES-1 for voltage regulation with input current control is demonstrated experimentally on a single-phase hardware setup. An ES with CSI is used in [39] for harmonic suppression. The harmonic distortion is shown to be reduced with CSI and direct current control. The harmonic components of the CL voltages can be suppressed further with the direct current control plus additional harmonics suppression function which is useful in high power systems. In [85], multiple resonant controllers and second-order generalized integrator are used for ES to suppress the harmonics and regulate the CL voltage. Wang *et al.* [86] use an improved PLL together with independent δ control in each phase to reduce unbalance and harmonic distortion in addition to stabilizing the mains voltage of the microgrid This is achieved by an improved PLL that separates the fundamental component of the positive sequence of the microgrid voltages from the other sequences and harmonics. An ES based on the neutral point clamped H-bridge inverter is shown to produce superior high-frequency harmonic suppression and improved total harmonic distortion in [87].

F. Unbalance Mitigation

In [24], a three-phase ES is used to reduce unbalance across a building making the building loads adaptive to internal load changes and external mains voltage changes. The experimental and simulation results show how the ES reduces unbalance by redistributing the power across the three phases of the NCL while regulating the mains voltages as usual. Mitigation of the negative-sequence and zero-sequence currents with ES-2 control based on the RCD approach is demonstrated in [36] and verified on a 3-kW hardware setup. The ES voltage injected in each phase is set to remove unbalance while minimizing the active power exchanged with the battery storage. In [88], a three-phase ES is considered for voltage regulation and reducing unbalance based on the theory of instantaneous power which is verified experimentally. Pawar *et al.* [37] use a modified instantaneous symmetrical component algorithm and hysteresis current control to operate ES in active power filter mode to mitigate harmonics and improve the power factor while regulating the mains voltage. The effectiveness of the proposed approach for ES-1 in achieving multiple functions is established through simulation and experiments. Moreover, the analysis presented in this article enables the integration of multiple control functions into the ES controller to achieve multiple objectives.

Liao *et al.* [64] use DCESs to mitigate unbalanced voltage and reduce power losses due to the neutral line current in a bipolar dc distribution network. The coupling between the positive- and negative-pole voltages is analyzed in addition to deriving the small-signal model of the bipolar dc distribution network with DCESs. The proposed unbalanced voltage suppression method and the decoupling control of DCESs are validated by simulations and experiments for resistive loads only. This is more complicated for constant-power loads and is not considered in this article.

G. System Resilience

Following extreme natural events, it is important to quickly restore the power supply, especially for the CLs. The role of ES in enhancing the resilience of a microgrid with intermittent renewable resources is shown in [89]. The voltages across the CLs are considered as a critical constraint for enhancing resilience during extreme natural events. Case studies presented demonstrate that ESs can enhance the resilience of microgrids with and without a communication system after extreme natural events. The ESs are shown to perform as expected with local information for the strong system, while communication is required to retain the same level of performance for weak systems.

H. System Stability

The impact of several ESs on the stability of the power grids is studied in [90]. The concept of relative stability is used to tune the gains of the PI controllers of the ES to ensure the overall system stability of a weak grid. A case study on the IEEE 13-node LV test feeder confirms that the constraints on controller gain become more stringent with an increasing number of ES to achieve system stability. Hence, the maximum number of ES can only be accommodated with the optimally chosen controller gains. Chakravorty *et al.* [67] present a small-signal stability analysis of the distribution networks with ES-1. The impact of distance of an ES from the substation, proximity between the adjacent ESs, and the

R/X ratio of the network on the small-signal stability of the system is analyzed and compared against the case with equivalent DG inverters. It is shown that ESs installed in the distribution networks are not likely to threaten the small-signal stability of the system. In fact, the stability margin with the ES installed is more than the case with equivalent penetration of shunt converters such as DG inverters.

In [91], the role of ES in damping low-frequency oscillations in a droop-controlled inverter-based microgrid is demonstrated. This is achieved by modulating the current of the ES based on the oscillations in the inverter reference frequency. The damping capability is shown to depend on the location of the ES. The presence of ES does not adversely affect the small-signal stability if appropriate control parameters are used. However, this is yet to be ascertained for weak grid situations considering different control modes of the ES.

In this section, the system-level impact of ES is summarized in terms of a variety of functionalities/services (e.g., voltage regulation, frequency control, power quality improvement) that it can offer. In practice, an ES might have to provide more than one of these services at different times for which an optimum scheduling mechanism has to be developed [92]. This would then enable a rigorous techno-economic value assessment of the ES technology considering multiple service provision which should further strengthen the business case for ES and expedite the uptake of the technology for mass deployment.

VII. Future Trends of ES

As reviewed in this article, the ES technology has evolved into various forms as fast and smart demand response technology for smart grids. Currently, several versions of ES (ES-1 and BTB ES) are being practically evaluated by China Southern Power Grid, Guangzhou, China [93]. While the ES circuits are initially associated with the NCLs together as SLs for DSM, it is worthwhile to consider the ES as part of the power supply infrastructure as illustrated in Fig. 32. The standard ac mains (with tight voltage tolerance) is regulated by the ES installed in the power supply infrastructure. The outputs of the ES form the adaptive ac mains (with a relatively large voltage tolerance). One business model is to offer discounts to the consumers when their NCLs consume electricity from the adaptive ac mains, because by doing so they are helping the power companies to stabilize the power grid and install more renewable energy sources.

Similar to individual mechanical springs, ESs can work independently without communication. This feature is very important because it ensures a large group of ESs to support the power grid in case the communication network fails. However, it does not mean that using distributed control in a cyber layer or communication network is irrelevant. In fact, more research is needed because distributed control of a large group of ESs distributed in the distribution network will likely offer many new functions that have not been explored. For examples, conduction power loss in a microgrid can be reduced [94] and overvoltage in a distribution network can be avoided [95]. Thus, there is a need for studying distributed control of ESs and also measures against cyberattacks of the distributed ES. While distributed control offers a new dimension of functions, ESs still provide their individual functions by reverting to droop control even if the cyber layer or distributed control fails.

With almost ten years of research and development and industry trial of ES underway, a cost–benefit analysis (CBA) of this technology is necessary to facilitate mass deployment. However, it is not straightforward to do a comprehensive and generalized CBA for an ES taking into account the multiple functionalities (e.g., voltage control, frequency regulation, power quality improvement) it can provide depending on the requirement at a given time. The proper value of an ES can be realized only when it is scheduled to provide multiple services (outlined in Section V) in conjunction with the competing alternatives (e.g., battery storage, STATCOM). Such a multiservice scheduling framework for ES is yet to be developed due to which the CBA and the associated payback calculation for ES are limited to sporadic attempts such as [17] focusing on a single service (e.g., frequency response) only. In addition, the requirement and value of these services will change depending on the penetration of renewables which varies a lot between countries/regions and anticipated future scenarios. Our ongoing research is aimed at firming up the CBA of ES for enhanced frequency response in GB for two 2030 scenarios.

VIII. Conclusion

This article reviews recent research and development of the ES technology and their applications in the smart grid. Similar to the mechanical springs for mechanical structures, ESs have been introduced to support and stabilize the power grid with increasing disturbances caused by high penetration of renewable energy sources of intermittent nature. So far, several versions of ES and their associated control strategies have been proposed and practically verified in microgrids. Besides mitigating mains voltage and frequency fluctuations, the ES also provides other auxiliary functions such as power quality improvement, reduction of power imbalance, and conduction power loss in power systems. The literature review shows that there is an increasing trend of studying a large group of distributed ESs in large-scale power systems. With ES reaching the stage of practical evaluation by the power industry, it is envisaged that the ES technology will offer a practical solution to speeding up the adoption of renewable energy sources without causing instability in the power grid to combat climate change.

References

[1] R. Lindsay. U.S. National Oceanic and Atmospheric Administration. (Dec. 10, 2019). *As Sea Ice Disappears, Arctic Seas Are Experience Extreme Summer Warmth*. [Online]. Available: https://www.climate.gov/news-features/featured-images/2019-arctic-report-card-sea-ice-disappears-arctic-seas-are

[2] M. Scott. U.S. National Oceanic and Atmospheric Administration. (Mar. 12, 2019). *Antarctica is Colder Than the Arctic, But it's Still Losing Ice*. [Online]. Available: https://www.climate.gov/news-features/features/antarctica-colder-arctic-it%E2%80%99s-still-losing-ice

[3] A. Borunda. Environment, National Geographic. (Aug. 29, 2019). *See How Much of the Amazon is Burning, How it Compares to Other Years*. [Online]. Available: https://www.nationalgeographic.com/environment/2019/08/amazon-fires-cause-deforestation-graphic-map/

[4] Nature Editorial, "Australia: Show the world what climate action looks like," *Nature*, vol. 577, pp. 449–450, Jan. 2020.

[5] *United State Environment Protection Agency Website*. Accessed: Jun. 26, 2020. [Online]. Available: https://www.epa.gov/

[6] International Renewable Energy Agency. (Mar. 31, 2019). *Renewable Capacity Highlights*. [Online]. Available: https://www.irena.org/publications/2019/Mar/Renewable-Capacity-Statistics-2019

[7] R. Fares. Scientific American. (Mar. 11, 2015). *Renewable Energy Intermittency Explained: Challenges, Solutions and Opportunities*. [Online]. Available: https://blogs.scientificamerican.com/plugged-in/renewable-energy-intermittency-explained-challenges-solutions-and-opportunities/

[8] Institute for Energy Research. (Jan. 23, 2013). *Germany's Green Energy Destabilizing Electric Grids*. [Online]. Available: https://www.instituteforenergyresearch.org/renewable/germanys-green-energy-destabilizing-electric-grids/

[9] P. Palensky and D. Dietrich, "Demand side management: Demand response, intelligent energy systems, and smart loads," *IEEE Trans. Ind. Informat.*, vol. 7, no. 3, pp. 381–388, Aug. 2011.

[10] S. Chen, P. Sinha, and N. B. Shroff, "Scheduling heterogeneous delay tolerant tasks in smart grid with renewable energy," in *Proc. IEEE 51st Conf. Decis. Control (CDC)*, Dec. 2012, pp. 1130–1135.

[11] K. Yang and A. Walid, "Outage-storage tradeoff in frequency regulation for smart grid with renewables," *IEEE Trans. Smart Grid*, vol. 4, no. 1, pp. 245–252, Mar. 2013.

[12] K. M. Tsui and S. C. Chan, "Demand response optimization for smart home scheduling under real-time pricing," *IEEE Trans. Smart Grid*, vol. 3, no. 4, pp. 1812–1821, Dec. 2012.

[13] E. Vrettos, C. Ziras, and G. Andersson, "Fast and reliable primary frequency reserves from refrigerators with decentralized stochastic control," *IEEE Trans. Power Syst.*, vol. 32, no. 4, pp. 2924–2941, Jul. 2017.

[14] R. Tonkoski, L. A. C. Lopes, and T. H. M. El-Fouly, "Coordinated active power curtailment of grid connected PV inverters for overvoltage prevention," *IEEE Trans. Sustain. Energy*, vol. 2, no. 2, pp. 139–147, Apr. 2011.

[15] Hooke's Law. *Britannica Online Encyclopedia*. Accessed: Jun. 26, 2020. [Online]. Available: http://www.britannica.com/EBchecked/topic/271336/Hookes-law

[16] S. Y. Hui, C. K. Lee, and F. F. Wu, "Electric springs—A new smart grid technology," *IEEE Trans. Smart Grid*, vol. 3, no. 3, pp. 1552–1561, Sep. 2012.

[17] J. Guo, B. Chaudhuri, and S. Y. R. Hui, "Flexible demand through point-of-load voltage control in domestic sector," *IEEE Trans. Smart Grid*, vol. 10, no. 4, pp. 4662–4672, Jul. 2019.

[18] EMSD. (2018). *Hong Kong Energy End-Use Data 2018*. [Online]. Available: https://www.emsd.gov.hk/filemanager/en/content_762/HKEEUD2018.pdf

[19] J. Soni, K. R. Krishnanand, and S. K. Panda, "Load-side demand management in buildings using controlled electric springs," in *Proc. 40th Annu. Conf. IEEE Ind. Electron. Soc. (IECON)*, Oct./Nov. 2014, pp. 5376–5381.

[20] C. K. Lee, B. Chaudhuri, and S. Y. Hui, "Hardware and control implementation of electric springs for stabilizing future smart grid with intermittent renewable energy sources," *IEEE J. Emerg. Sel. Topics Power Electron.*, vol. 1, no. 1, pp. 18–27, Mar. 2013.

[21] E. F. Areed, M. A. Abido, and A. T. Al-Awami, "Switching model analysis and implementation of electric spring for voltage regulation in smart grids," *IET Gener., Transmiss. Distrib.*, vol. 11, no. 15, pp. 3703–3712, Oct. 2017.

[22] X. Chen, Y. Hou, S. C. Tan, C. K. Lee, and S. Y. R. Hui, "Mitigating voltage and frequency fluctuation in microgrids using electric springs," *IEEE Trans. Smart Grid*, vol. 6, no. 2, pp. 508–515, Mar. 2015.

[23] Q. Wang, M. Cheng, Z. Chen, and Z. Wang, "Steady-state analysis of electric springs with a novel δ control," *IEEE Trans. Power Electron.*, vol. 30, no. 12, pp. 7159–7169, Dec. 2015.

[24] S. Yan, S.-C. Tan, C.-K. Lee, B. Chaudhuri, and S. Y. R. Hui, "Electric springs for reducing power imbalance in three-phase power systems," *IEEE Trans. Power Electron.*, vol. 30, no. 7, pp. 3601–3609, Jul. 2015.

[25] C. Yuan, J. Feng, M. Tong, D. Yang, and N. Tang, "Piecewise control strategy for electric spring," *IET Gener., Transmiss. Distribution*, vol. 13, no. 12, pp. 2496–2506, Jun. 2019.

[26] C. Yuan, M. Tong, J. Feng, and R. Zhou, "Control of electric spring for frequency regulation," *J. Eng.*, vol. 2019, no. 16, pp. 2500–2504, Mar. 2019.

[27] S.-C. Tan, C. K. Lee, and S. Y. Hui, "General steady-state analysis and control principle of electric springs with active and reactive power compensations," *IEEE Trans. Power Electron.*, vol. 28, no. 8, pp. 3958–3969, Aug. 2013.

[28] Z. Zhao, K. Wang, S. Yang, G. Li, and Y. Zhang, "Research on optimal operation of distribution network with electric springs," *J. Eng.*, vol. 2019, no. 16, pp. 2953–2956, Mar. 2019.

[29] T. Yang, K.-T. Mok, S.-C. Tan, C. Kwan Lee, and S. Yuen Hui, "Electric springs with coordinated battery management for reducing voltage and frequency fluctuations in microgrids," *IEEE Trans. Smart Grid*, vol. 9, no. 3, pp. 1943–1952, May 2018.

[30] S. Yan *et al.*, "Extending the operating range of electric spring using back-to-back converter: Hardware implementation and control," *IEEE Trans. Power Electron.*, vol. 32, no. 7, pp. 5171–5179, Jul. 2017.

[31] D. Chakravorty, B. Chaudhuri, and S. Y. R. Hui, "Rapid frequency response from smart loads in great britain power system," *IEEE Trans. Smart Grid*, vol. 8, no. 5, pp. 2160–2169, Sep. 2017.

[32] H. Liu, W. M. Ng, C.-K. Lee, and S. Y. Ron Hui, "Integration of flexible loads and electric spring using a three-phase inverter," *IEEE Trans. Power Electron.*, vol. 35, no. 8, pp. 8013–8024, Aug. 2020.

[33] T. Yang, K.-T. Mok, S.-S. Ho, S.-C. Tan, C.-K. Lee, and R. S. Y. Hui, "Use of integrated photovoltaic-electric spring system as a power balancer in power distribution networks," *IEEE Trans. Power Electron.*, vol. 34, no. 6, pp. 5312–5324, Jun. 2019.

[34] A. K. Khamis, N. E. Zakzouk, A. K. Abdelsalam, and A. A. Lotfy, "Decoupled control strategy for electric springs: Dual functionality feature," *IEEE Access*, vol. 7, pp. 57725–57740, Apr. 2019.

[35] M.-H. Wang, T.-B. Yang, S.-C. Tan, and S. Y. Hui, "Hybrid electric springs for grid-tied power control and storage reduction in AC microgrids," *IEEE Trans. Power Electron.*, vol. 34, no. 4, pp. 3214–3225, Apr. 2019.

[36] K.-T. Mok, S.-S. Ho, S.-C. Tan, and S. Y. Hui, "A comprehensive analysis and control strategy for nullifying Negative- and zero-sequence currents in an unbalanced three-phase power system using electric springs," *IEEE Trans. Power Electron.*, vol. 32, no. 10, pp. 7635–7650, Oct. 2017.

[37] R. S. Pawar, S. P. Gawande, R. N. Nagpure, and M. A. Waghmare, "Modified instantaneous symmetrical component algorithm-based control for operating electric spring in active power filter mode," *IET Power Electron.*, vol. 12, no. 7, pp. 1730–1741, Jun. 2019.

[38] A. Rauf, V. Khadkikar, and M. Elmoursi, "An integrated system configuration for electric springs to enhance the stability in future smart grid," presented at the Mod. Electr. Power Syst., Wroclaw, Poland, Jul. 6–9, 2015.

[39] Q. Wang, M. Cheng, and Y. Jiang, "Harmonics suppression for critical loads using electric springs with current-source inverters," *IEEE J. Emerg. Sel. Topics Power Electron.*, vol. 4, no. 4, pp. 1362–1369, Dec. 2016.

[40] X. Luo, Z. Akhtar, C. K. Lee, B. Chaudhuri, S.-C. Tan, and S. Y. R. Hui, "Distributed voltage control with electric springs: Comparison with STATCOM," *IEEE Trans. Smart Grid*, vol. 6, no. 1, pp. 209–219, Jan. 2015.

[41] S. Yan, S.-C. Tan, C.-K. Lee, B. Chaudhuri, and S. Y. R. Hui, "Use of smart loads for power quality improvement," *IEEE J. Emerg. Sel. Topics Power Electron.*, vol. 5, no. 1, pp. 504–512, Mar. 2017.

[42] Q. Wang, M. Cheng, Z. Chen, and Z. Wang, "Steady-state analysis of electric springs with a novel δ control," *IEEE Trans. Power Electron.*, vol. 30, no. 12, pp. 7159–7169, Dec. 2015.

[43] Q. Wang, M. Cheng, Y. Jiang, W. Zuo, and G. Buja, "A simple active and reactive power control for applications of single-phase electric springs," *IEEE Trans. Ind. Electron.*, vol. 65, no. 8, pp. 6291–6300, Aug. 2018.

[44] Q. Wang, Z. Ding, M. Cheng, F. Deng, and G. Buja, "A parameter-exempted, high-performance power decoupling control of single-phase electric springs," *IEEE Access*, vol. 8, pp. 33370–33379, Feb. 2020.

[45] Y. Mohamed and E. F. El-Saadany, "Adaptive decentralized droop controller to preserve power sharing stability of paralleled inverters in distributed generation microgrids," *IEEE Trans. Power Electron.*, vol. 23, no. 6, pp. 2806–2816, Nov. 2008.

[46] M. Fakhari Moghaddam Arani and Y. A.-R.-I. Mohamed, "Dynamic droop control for wind turbines participating in primary frequency regulation in microgrids," *IEEE Trans. Smart Grid*, vol. 9, no. 6, pp. 5742–5751, Nov. 2018.

[47] C. K. Lee, N. R. Chaudhuri, B. Chaudhuri, and S. Y. R. Hui, "Droop control of distributed electric springs for stabilizing future power grid," *IEEE Trans. Smart Grid*, vol. 4, no. 3, pp. 1558–1566, Sep. 2013.

[48] Z. Akhtar, B. Chaudhuri, and S. Yuen Ron Hui, "Smart loads for voltage control in distribution networks," *IEEE Trans. Smart Grid*, vol. 8, no. 2, pp. 937–946, Mar. 2017.

[49] Z. Akhtar, B. Chaudhuri, and S. Y. R. Hui, "Primary frequency control contribution from smart loads using reactive compensation," *IEEE Trans. Smart Grid*, vol. 6, no. 5, pp. 2356–2365, Sep. 2015.

[50] G. Chen, F. L. Lewis, E. N. Feng, and Y. Song, "Distributed optimal active power control of multiple generation systems," *IEEE Trans. Ind. Electron.*, vol. 62, no. 11, pp. 7079–7090, Nov. 2015.

[51] M. Zeraati, M. E. Hamedani Golshan, and J. M. Guerrero, "A consensus-based cooperative control of PEV battery and PV active power curtailment for voltage regulation in distribution networks," *IEEE Trans. Smart Grid*, vol. 10, no. 1, pp. 670–680, Jan. 2019.

[52] J. Khazaei and Z. Miao, "Consensus control for energy storage systems," *IEEE Trans. Smart Grid*, vol. 9, no. 4, pp. 3009–3017, Jul. 2018.

[53] J. Chen, S. Yan, and S. Y. R. Hui, "Using consensus control for reactive power sharing of distributed electric springs," in *Proc. IEEE Energy Convers. Congr. Expo.*, Oct. 2017, pp. 3741–3746.

[54] Y. Zheng, D. J. Hill, K. Meng, and S. Y. Hui, "Critical bus voltage support in distribution systems with electric springs and responsibility sharing," *IEEE Trans. Power Syst.*, vol. 32, no. 5, pp. 3584–3593, Sep. 2017.

[55] J. Chen, S. Yan, T. Yang, S.-C. Tan, and S. Y. Hui, "Practical evaluation of droop and consensus control of distributed electric springs for both voltage and frequency regulation in microgrid," *IEEE Trans. Power Electron.*, vol. 34, no. 7, pp. 6947–6959, Jul. 2019.

[56] K. T. Mok, M. H. Wang, S. C. Tan, and S. Y. R. Hui, "DC electric springs—A new technology for stabilizing DC power distribution systems," *IEEE Trans. Power Electron.*, vol. 32, no. 2, pp. 1088–1104, Feb. 2017.

[57] M.-H. Wang, K.-T. Mok, S.-C. Tan, and S. Y. Hui, "Multifunctional DC electric springs for improving voltage quality of DC grids," *IEEE Trans. Smart Grid*, vol. 9, no. 3, pp. 2248–2258, May 2018.

[58] M.-H. Wang, S. Yan, S.-C. Tan, and S. Y. Hui, "Hybrid-DC electric springs for DC voltage regulation and harmonic cancellation in DC microgrids," *IEEE Trans. Power Electron.*, vol. 33, no. 2, pp. 1167–1177, Feb. 2018.

[59] Q. Wang, D. Zha, F. Deng, M. Cheng, and G. Buja, "A topology of DC electric springs for DC household applications," *IET Power Electron.*, vol. 12, no. 5, pp. 1241–1248, May 2019.

[60] Y. Yang, S.-C. Tan, and S. Y. R. Hui, "Mitigating distribution power loss of DC microgrids with DC electric springs," *IEEE Trans. Smart Grid*, vol. 9, no. 6, pp. 5897–5906, Nov. 2018.

[61] M.-H. Wang, S. Yan, S.-C. Tan, Z. Xu, and S. Y. Hui, "Decentralized control of DC electric springs for storage reduction in DC microgrids," *IEEE Trans. Power Electron.*, vol. 35, no. 5, pp. 4634–4646, May 2020.

[62] X. Chen, M. Shi, H. Sun, Y. Li, and H. He, "Distributed cooperative control and stability analysis of multiple DC electric springs in a DC microgrid," *IEEE Trans. Ind. Electron.*, vol. 65, no. 7, pp. 5611–5622, Jul. 2018.

[63] D. Zha, Q. Wang, M. Cheng, F. Deng, and G. Buja, "Distributed cooperative control for multiple DC electric springs with novel topologies applied in DC microgrid," in *Proc. IEEE 10th Int. Symp. Power Electron. Distrib. Gener. Syst. (PEDG)*, Jun. 2019, pp. 648–652.

[64] J. Liao, N. Zhou, Y. Huang, and Q. Wang, "Unbalanced voltage suppression in a bipolar DC distribution network based on DC electric springs," *IEEE Trans. Smart Grid*, vol. 11, no. 2, pp. 1667–1678, Mar. 2020.

[65] N. R. Chaudhuri, C. K. Lee, B. Chaudhuri, and S. Y. R. Hui, "Dynamic modeling of electric springs," *IEEE Trans. Smart Grid*, vol. 5, no. 5, pp. 2450–2458, Sep. 2014.

[66] T. Yang, T. Liu, J. Chen, S. Yan, and S. Y. R. Hui, "Dynamic modular modeling of smart loads associated with electric springs and control," *IEEE Trans. Power Electron.*, vol. 33, no. 12, pp. 10071–10085, Dec. 2018.

[67] D. Chakravorty, J. Guo, B. Chaudhuri, and S. Y. R. Hui, "Small signal stability analysis of distribution networks with electric springs," presented at the IEEE Power Energy Soc. Gen. Meeting, Aug. 5–10, 2018.

[68] D. Zha, Q. Wang, M. Cheng, and F. Deng, "Energy management system applied in DC electric springs," in *Proc. 10th Int. Conf. Power Electron. (ECCE) Asia*, May 2019, pp. 1435–1439.

[69] Z. Akhtar, M. Opatovsky, B. Chaudhuri, and S. Y. R. Hui, "Comparison of point-of-load versus mid-feeder compensation in LV distribution networks with high penetration of solar photovoltaic generation and electric vehicle charging stations," *IET Smart Grid*, vol. 2, no. 2, pp. 283–292, Jun. 2019.

[70] Y. Zheng, C. Zhang, D. J. Hill, and K. Meng, "Consensus control of electric spring using back-to-back converter for voltage regulation with ultra-high renewable penetration," *J. Mod. Power Syst. Clean Energy*, vol. 5, no. 6, pp. 897–907, Nov. 2017.

[71] Y. Zheng, D. J. Hill, Y. Song, J. Zhao, and S. Y. R. Hui, "Optimal electric spring allocation for risk-limiting voltage regulation in distribution systems," *IEEE Trans. Power Syst.*, vol. 35, no. 1, pp. 273–283, Jan. 2020.

[72] Y. Zheng, W. Kong, Y. Song, and D. J. Hill, "Optimal operation of electric springs for voltage regulation in distribution systems," *IEEE Trans. Ind. Informat.*, vol. 16, no. 4, pp. 2551–2561, Apr. 2020.

[73] M. Askarpour, J. Aghaei, J. Boudjadar, and T. Niknam, "Techno-economic potential gains of electric springs in distribution networks operations," *IET Gener., Transmiss. Distrib.*, vol. 14, no. 1, pp. 98–107, Jan. 2020.

[74] H. Zhao, J. Zhao, Y. Zheng, J. Qiu, and F. Wen, "A hybrid method for electric spring control based on data and knowledge integration," *IEEE Trans. Smart Grid*, vol. 11, no. 3, pp. 2303–2312, May 2020.

[75] L. Liang, Y. Hou, and D. J. Hill, "Enhancing flexibility of an islanded microgrid with electric springs," *IEEE Trans. Smart Grid*, vol. 10, no. 1, pp. 899–909, Jan. 2019.

[76] M. S. Pilehvar, M. B. Shadmand, and B. Mirafzal, "Analysis of smart loads in nanogrids," *IEEE Access*, vol. 7, pp. 548–562, 2019.

[77] L. Liang, Y. Hou, and D. J. Hill, "An interconnected microgrids-based transactive energy system with multiple electric springs," *IEEE Trans. Smart Grid*, vol. 11, no. 1, pp. 184–193, Jan. 2020.

[78] T. Liu, D. J. Hill, and C. Zhang, "Non-disruptive load-side control for frequency regulation in power systems," *IEEE Trans. Smart Grid*, vol. 7, no. 4, pp. 2142–2153, Jul. 2016.

[79] C. Zhang, T. Liu, S. Yan, and D. J. Hill, "Granular load-side frequency control with electric spring aggregators and leader–follower consensus," *IET Gener., Transmiss. Distrib.*, vol. 13, no. 9, pp. 1700–1708, May 2019.

[80] K. Schneider, F. Tuffner, J. Fuller, and R. Singh. (2010). *Evaluation of Conservation Voltage Reduction (CVR) on a National Level*. [Online]. Available: https://www.pnnl.gov/main/publications/external/technical_reports/PNNL-19596.pdf

[81] A. Ballanti and L. F. Ochoa, "Voltage-led load management in whole distribution networks," *IEEE Trans. Power Syst.*, vol. 33, no. 2, pp. 1544–1554, Mar. 2018.

[82] G. De Carne, G. Buticchi, M. Liserre, and C. Vournas, "Real-time primary frequency regulation using load power control by smart transformers," *IEEE Trans. Smart Grid*, vol. 10, no. 5, pp. 5630–5639, Sep. 2019.

[83] T. Chen, J. Guo, B. Chaudhuri, and R. S. Y. Hui, "Virtual inertia from smart loads," *IEEE Trans. Smart Grid*, early access, Apr. 2020, doi: 10.1109/TSG.2020.2988444.

[84] D. Chakravorty, B. Chaudhuri, and S. Y. R. Hui, "Estimation of aggregate reserve with point-of-load voltage control," *IEEE Trans. Smart Grid*, vol. 9, no. 5, pp. 4649–4658, Sep. 2018.

[85] P. Kanjiya and V. Khadkikar, "Enhancing power quality and stability of future smart grid with intermittent renewable energy sources using electric springs," presented at the Int. Conf. Renew. Energy Res. Appl., Oct. 20–23, 2013.

[86] Q. Wang, M. Cheng, Y. Jiang, F. Deng, Z. Chen, and G. Buja, "Control of three-phase electric springs used in microgrids under ideal and non-ideal conditions," in *Proc. IECON 42nd Annu. Conf. IEEE Ind. Electron. Soc.*, Oct. 2016, pp. 2247–2252.

[87] K. Gajbhiye, P. Dahiwale, S. Bharti, R. Pawar, S. P. Gawande, and S. G. Kadwane, "Five-level NPC/H-bridge MLI based electric spring for harmonic reduction and voltage regulation," in *Proc. Int. Conf. Smart Grids, Power Adv. Control Eng. (ICSPACE)*, Aug. 2017, pp. 203–208.

[88] S. Yan, M.-H. Wang, T.-B. Yang, S.-C. Tan, B. Chaudhuri, and S. Y. R. Hui, "Achieving multiple functions of three-phase electric springs in unbalanced three-phase power systems using the instantaneous power theory," *IEEE Trans. Power Electron.*, vol. 33, no. 7, pp. 5784–5795, Jul. 2018.

[89] L. Liang, Y. Hou, D. J. Hill, and S. Yuen Ron Hui, "Enhancing resilience of microgrids with electric springs," *IEEE Trans. Smart Grid*, vol. 9, no. 3, pp. 2235–2247, May 2018.

[90] Y. Yang, S.-S. Ho, S.-C. Tan, and S.-Y.-R. Hui, "Small-signal model and stability of electric springs in power grids," *IEEE Trans. Smart Grid*, vol. 9, no. 2, pp. 857–865, Mar. 2018.
[91] A. Firdaus, S. Mishra, and D. Sharma, "Stability enhancement of inverter based autonomous microgrid using electric spring," in *Proc. IEEE Int. Conf. Environ. Electr. Eng. Ind. Commercial Power Syst. Eur. (EEEIC/I&CPS Eur.)*, Jun. 2019, pp. 1–5.
[92] T. Chen, H. Liu, C.-K. Lee, and S. Y. R. Hui, "A generalized controller for electric-spring-based smart load with both active and reactive power compensation," *IEEE J. Emerg. Sel. Topics Power Electron.*, vol. 8, no. 2, pp. 1454–1465, Jun. 2020.
[93] N. Tang, K. Yang, H. Huang, and C. K. Lee, "The application of one-cycle control technology in electric spring system," *IOP Conf. Ser. Earth Environ. Sci.*, vol. 170, no. 4, 2018, Art. no. 042117.
[94] Y. Yang, Y. Qin, S.-C. Tan, and S. Y. Hui, "Reducing distribution power loss of islanded AC microgrids using distributed electric springs with predictive control," *IEEE Trans. Ind Electron*, early access, Feb. 2020, doi: 10.1109/TIE.2020.2972450.
[95] T. Chen, Y. Zheng, B. Chaudhuri, and S. Y. R. Hui, "Distributed electric-spring-based smart thermal loads for overvoltage prevention in LV distributed network using dynamic consensus approach," *IEEE Trans. Sustain. Energy*, early access, Oct. 2020, doi: 10.1109/TSTE.2019.2950421.

Chi-Kwan Lee (Senior Member, IEEE) received the B.Eng. and Ph.D. degrees in electronic engineering from the City University of Hong Kong, Hong Kong, in 1999 and 2004, respectively.

He is currently an Associate Professor with the Department of Electrical and Electronic Engineering, The University of Hong Kong, Hong Kong. Since 2010, he has been a Visiting Researcher with Imperial College London, London, U.K. He is a Co-Inventor of the electric springs. His current research interests include wireless power transfer and clean energy technologies.

Dr. Lee received the IEEE POWER ELECTRONICS TRANSACTIONS First Prize Paper Award for his publications on mid-range wireless power transfer in 2015.

Heng Liu received the B.Eng. and M.Phil. degrees in electrical engineering from Zhejiang University, Hangzhou, China, in 2011 and 2014, and the Ph.D. degree in electrical and electronic engineering from The University of Hong Kong, Hong Kong, in 2019.

Her research interest includes smart grid and power electronic technologies.

Siew-Chong Tan (Senior Member, IEEE) received the B.Eng. (Hons.) and M.Eng. degrees in electrical and computer engineering from the National University of Singapore, Singapore, in 2000 and 2002, respectively, and the Ph.D. degree in electronic and information engineering from Hong Kong Polytechnic University, Hong Kong, in 2005.

He was a Visiting Scholar with the Grainger Center for Electric Machinery and Electromechanics, University of Illinois at Urbana–Champaign, Champaign, IL, USA, from September 2009 to October 2009, and an Invited Academic Visitor with the Huazhong University of Science and Technology, Wuhan, China, in December 2011. He is currently a Professor with the Department of Electrical and Electronic Engineering, The University of Hong Kong, Hong Kong. His research interests are focused in the areas of power electronics and control, LED lightings, smart grids, and clean energy technologies.

Balarko Chaudhuri (Senior Member, IEEE) received the Ph.D. degree in electrical and electronic engineering from Imperial College London, London, U.K., in 2005.

He is currently a Reader of power systems with Imperial College London. His research interests include power systems dynamics and stability, grid integration of renewable energy, wide-area control through HVdc/FACTS, and demand response.

Dr. Chaudhuri is a fellow of the Institution of Engineering and Technology (IET). He serves as an Editor for the IEEE TRANSACTIONS ON SMART GRID and an Associate Editor for the IEEE SYSTEMS JOURNAL and *Elsevier Control Engineering Practice*.

Shu-Yuen Ron Hui (Fellow, IEEE) received the B.Sc. (Eng) degree (Hons.) in electrical and electronic engineering from the University of Birmingham, Birmingham, U.K., in 1984, and the D.I.C. and Ph.D. degrees in electrical engineering from Imperial College London, London, U.K., in 1987.

He is currently a Chair Professor of power electronics with The University of Hong Kong, Hong Kong, and Imperial College London. His research interests include power electronics, wireless power, sustainable lighting, and smart grid. His inventions on wireless charging platform technology underpin key dimensions of Qi, the world's first wireless power standard, with freedom of positioning and localized charging features for wireless charging of consumer electronics. He also developed the photo-electro-thermal theory for LED systems and co-invented electric springs.

Dr. Hui is a fellow of the Australian Academy of Technology and Engineering, the U.S. National Academy of Inventors, and the Royal Academy of Engineering, U.K. He received the IEEE Rudolf Chope Research and Development Award and the IET Achievement Medal (The Crompton Medal) in 2010 and the IEEE William E. Newell Power Electronics Award in 2015.